



AALBORG UNIVERSITY
DENMARK

Aalborg Universitet

The vascular integrity of the brain in chronic neurodegeneration

Thomsen, Maj Schneider

DOI (link to publication from Publisher):
[10.5278/vbn.phd.med.00039](https://doi.org/10.5278/vbn.phd.med.00039)

Publication date:
2015

Document Version
Publisher's PDF, also known as Version of record

[Link to publication from Aalborg University](#)

Citation for published version (APA):
Thomsen, M. S. (2015). The vascular integrity of the brain in chronic neurodegeneration. Aalborg Universitetsforlag. (Ph.d.-serien for Det Sundhedsvidenskabelige Fakultet, Aalborg Universitet). DOI: 10.5278/vbn.phd.med.00039

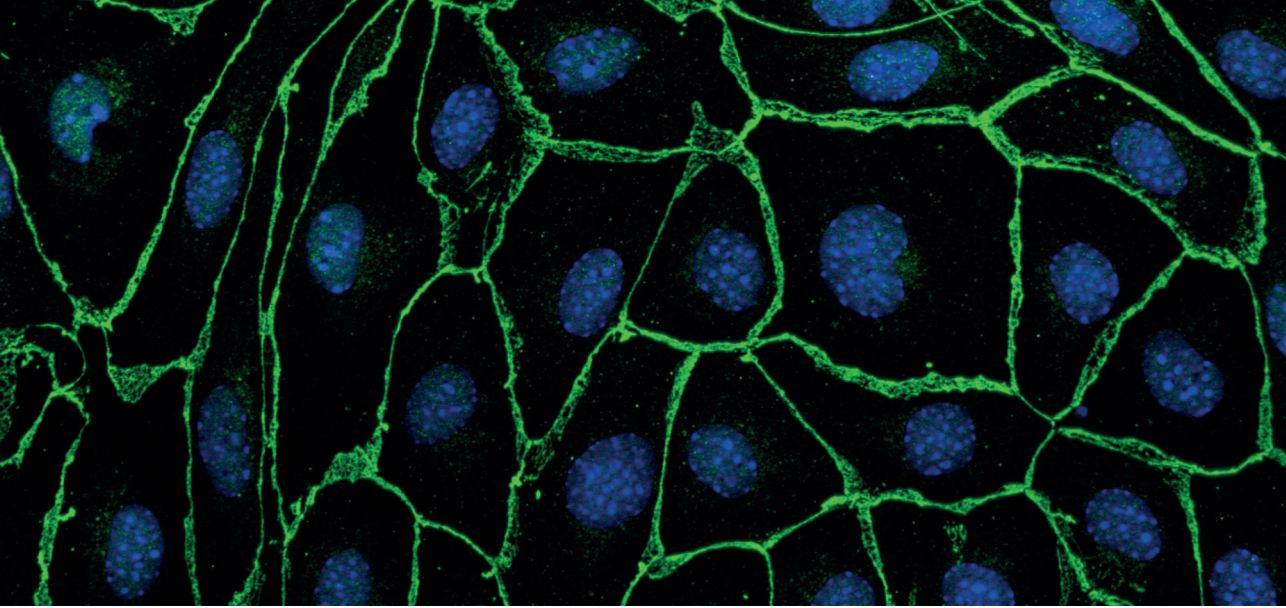
General rights

Copyright and moral rights for the publications made accessible in the public portal are retained by the authors and/or other copyright owners and it is a condition of accessing publications that users recognise and abide by the legal requirements associated with these rights.

- ? Users may download and print one copy of any publication from the public portal for the purpose of private study or research.
- ? You may not further distribute the material or use it for any profit-making activity or commercial gain
- ? You may freely distribute the URL identifying the publication in the public portal ?

Take down policy

If you believe that this document breaches copyright please contact us at vbn@aub.aau.dk providing details, and we will remove access to the work immediately and investigate your claim.



**THE VASCULAR INTEGRITY OF THE BRAIN
IN CHRONIC NEURODEGENERATION**

**BY
MAJ SCHNEIDER THOMSEN**

DISSERTATION SUBMITTED 2015



AALBORG UNIVERSITY
DENMARK

THE VASCULAR INTEGRITY OF THE BRAIN IN CHRONIC NEURODEGENERATION

Maj Schneider Thomsen



AALBORG UNIVERSITY
DENMARK

PhD-Dissertation submitted December 2015

Thesis submitted: December, 2015

PhD supervisor: Professor Torben Moos
Laboratory of Neurobiology
Department of Health Science and Technology
Aalborg University

PhD committee: Dr. Cristian Pablo Pennisi (chairman)
Aalborg University, DK

Dr. David J. Begley
King's College London, UK

Dr. Kate Lykke Lambertsen
University of Southern Denmark, DK

PhD Series: Faculty of Medicine, Aalborg University

ISSN (online): 2246-1302
ISBN (online): 978-87-7112-446-0

Published by:
Aalborg University Press
Skjernvej 4A, 2nd floor
DK – 9220 Aalborg Ø
Phone: +45 99407140
aauf@forlag.aau.dk
forlag.aau.dk

© Copyright: Maj Schneider Thomsen

Printed in Denmark by Rosendahls, 2015

CURRICULUM VITAE

Maj Schneider Thomsen
Dalgasgade 21, 3th
9000 Aalborg
+45 23440761
mst@hst.aau.dk



EDUCATION

Cand.scient.med Medicine with industrial specialization, Biomedicine, Aalborg University Master thesis: <i>Protective and Toxic Proteins in Alzheimer's Disease, Composed at University of Otago, New Zealand, with Professor Warren Tate</i>	2010-2012
B.Sc. Medicine with Industrial Specialization, Aalborg University	2007-2010

WORK EXPERIENCE

Research assistant at the Laboratory of Neurobiology, Aalborg University	2015-now
PhD student at the Laboratory of Neurobiology, Aalborg University	2012-2015
Research assistant at the Laboratory for stem cell research, Aalborg University	Feb 2011- June 2011

CONFERENCES

Barriers of the CNS – Presentation of poster	June 2014
Brain4Brains 8th plenary meeting	March 2014
Aarhus CTTH workshop 2013 – Presentation of poster	December 2013
The 10th international Conference on Cerebral Vascular Biology	June 2013
3xRIBDD biannual workshop –Presentation of poster	2014 and 2015

TEACHING EXPERIENCE

Project supervisor 4th and 6th semester Medis/Medicine
Case facilitator 3rd and 4th semester Medis/Medicine
Histology Assistant t1st semester Medis/Medicine
Lectures – Dementia 5th semester Medis/Medicine
Mentor for at student with Asperger's syndrome

FUNDING

Fonden for Lægevidenskabens fremme	December 2014
------------------------------------	---------------

ENGLISH SUMMARY

The central nervous system (CNS) is protected from the circulation by two distinct barriers: the blood-brain barrier (BBB) and the blood-cerebrospinal fluid barrier. These barriers protect the brain by limiting the entry of toxins, pathogens, and many molecules circulating in the blood. The BBB is located at the brain's microvasculature and consists of specialised brain capillary endothelial cells (BCECs), which are tightly connected through so-called tight junction proteins. The specialised endothelial cells are supported by pericytes embedded in the vascular basement membrane and astrocyte endfeet. Interaction between the components of BBB is of utmost importance for proper function of the BBB.

The protection of the brain by the BBB from unwanted substances circulating in the blood is under normal physiological circumstances of great value for maintaining a healthy brain environment. However, in the case of brain diseases the barrier becomes an obstacle for the delivery of drugs to the CNS, and much research has gone into finding a way to pass this barrier. Furthermore, it is now well recognised that in condition with chronic neurodegeneration and inflammation such as Alzheimer's disease, Parkinson's disease, and multiple sclerosis, changes of the BBB are often observed. These changes include increased BBB permeability, neoangiogenesis, changed expression of tight junction proteins, and basement membrane thickening. This PhD-thesis is based on four papers in which the BBB is investigated under normal physiological conditions (Study I and II) and during chronic neurodegeneration with inflammation (Study III and IV).

Models of the BBB are useful tools for investigation of the responses of the BBB to various insults. In study I, a murine BBB model was established and investigated for the expression of basement membrane proteins. Murine BCECs (mBCECs), pericytes, and mixed glial cells were isolated and grown in four different experimental setups consisting of: mBCECs grown in mono-culture, and in co-culture with pericytes or mixed glial cells, or in triple-culture with both pericytes and mixed glial cells. The mBCECs grown in co- and triple-cultures have significant higher transendothelial electrical resistance (TEER) compared to the mono-culture. The contribution of the mBCECs to the synthesis of basement membrane proteins was investigated

with RT-qPCR, mass spectrometry, and immunofluorescence. The mBCECs expressed many major basement membrane proteins, and the gene expressions of laminin $\alpha 5$ and collagen IV were affected by the culture conditions. In study II, the co-culture with mBCECs and mixed glial cells was investigated for the expression of the neonatal Fc receptor (FcRn), which is believed to be involved in the transport of IgG from brain to blood. It was concluded that FcRn is indeed expressed albeit at low levels by the mBCECs.

A rat model of neurodegeneration with inflammation was created by injection of the glutamate agonist ibotenic acid into the striatum. Subsequently, this led to death among GABAergic neurons projecting to substantia nigra pars reticulata (SNpr), thereby creating an imbalance between the glutamate projections from nucleus subthalamicus and the GABAergic projections from striatum to SNpr. This resulted in overstimulation of the neurons in SNpr, which eventually caused excitotoxic-induced death among the neurons in SNpr. In study III, the inflammatory process in response to excitotoxic neuronal death in SNpr was investigated, together with the handling of the increasing amount of iron, which accompanies the infiltration of inflammatory cells. The study revealed that the neurodegeneration with inflammation was prominent and ongoing even at post-surgery day 91. Therefore, the main purpose of study IV was to investigate changes of the BBB permeability, expression of basement membrane proteins and adhesion molecules in response to the induced chronic neurodegeneration with inflammation. To further investigate the response of the BBB to inflammation, a rat triple-culture model of the BBB was established and exposed to lipopolysaccharide (LPS). Increased BBB permeability was observed by the presence of a prominent albumin immunoreaction in the SNpr. In addition, an increased gene expression of both intercellular adhesion molecule 1 (*Icam1*) and tissue inhibitor of metalloproteinases 1 (*Timp1*) were observed in the *in vivo* model of chronic neurodegenerative with inflammation and in the *in vitro* BBB model in response to LPS exposure. *In vitro*, the increased expression of *Icam1* was observed among BCECs and astrocytes, whereas the increased expression of *Timp1* was observed in pericytes and astrocytes. This indicates that these cell types contribute to the increased gene expression of *Icam1* and *Timp1* *in vivo* in response to excitotoxic-mediated neuronal death in SNpr.

DANSK RESUME

To forskellige barrierer adskiller centralnervesystemet (CNS) fra det cirkulerende blod: Blod-hjernebarrieren (eng. blood-brain barrier (BBB)) og blod-cerebrospinalvæskebarrieren. Disse to barrierer beskytter hjernen ved at forhindre, at skadelige stoffer fra blodbanen kan komme ind i hjernevævet. BBB er lokaliseret i hjernens kapillærer og består af specialiserede hjernekapillærendotelceller (eng. Brain capillary endothelial cells (BCECs)), som er tæt forbundet af såkaldt ”tight junction”-proteiner. BCECs understøttes af pericytten, som er indlejret i den vaskulære basalmembran og astrocyt endefødder. Samspelet mellem BCEC, pericyt og astrocyt er vigtig for, at denne barriere kan opretholdes.

BBB beskytter som sagt hjernen imod skadelige stoffer cirkulerende i blodbanen. Dette er under normale fysiologiske omstændigheder en fordel, men ved forskellige neurologiske sygdomme i CNS bliver denne barriere en forhindring for leveringen af lægemidler, hvorfor en del forskning har adresseret dette problem og prøvet at finde måder, hvorpå denne barriere kan passeres. Ydermere er det nu vist i flere studier, at BBB ændres ved neurodegenerative sygdomme med inflammation som f.eks. Alzheimers sygdom, Parkinsons sygdom og multiple sklerose. Disse ændringer inkluderer blandt andet øget BBB permeabilitet, neoangiogenese, ændret ekspresion af ”tight junction”-proteiner og fortykket basalmembran. Disse ændringer formodes at kunne øge lægemiddelleveringen til CNS. Ph.d. afhandlingen er baseret på fire studier, hvor forskellige aspekter af BBBen undersøges under normale fysiologiske omstændigheder (studie I og II) samt ved kronisk neurodegeneration med inflammation (studie III og IV).

In vitro BBB modeller er brugbare i forhold til at studere interaktion mellem de forskellige celler, som udgør BBB eller responset på forskellige stimuli. Begge undersøgelser ville være hen imod umulige at studere *in vivo*. Formålet med første studie var derfor at etablere en *in vitro* model for den murine BBB. murine BCECs (mBCECs), pericytter og en kultur af blandede gliaceller blev isoleret fra hjerner fra mus og groet i fire forskellige setups bestående af: mBCECs groet i monokultur, i co-kultur med pericytter eller blandede gliaceller eller i triple-kultur med både pericytter og blandede gliaceller. Både co- og triple-kulturerne havde signifikant højere transendothel elektrisk resistent (TEER) i forhold til mono-kulturen.

Derudover blev mBCECs bidrag til basalmembranen undersøgt med RT-qPCR, massespektrometri og immunofluorescens. mBCECs producerede forskellige basalmembran protein *in vitro* og gen-ekspressionen af både laminin $\alpha 5$ og collagen IV $\alpha 1$ var påvirket af dyrkningsforholdene. I studie II blev co-kulturen med mBCECs og blandede gliaceller undersøgt for udtrykket af neonatal Fc receptoren (FcRn), da denne receptor menes at være involveret i transport af IgG fra hjerne til blod. Det blev konkluderet at mBCECs har et lavt udtryk af FcRn.

En rottemodel for kronisk neurodegeneration med inflammation blev induceret ved at injicere glutamat agonisten ibotensyre i striatum. Dette medfører, at mange af de GABAerge neuroner, der projicerer til substantia nigra pars reticulata (SNpr), dør, og derved skabes der en ubalance mellem glutamat projektionerne fra nucleus subthalamicus til SNpr og de GABAerge projektioner fra striatum. Resultatet af denne ubalance er, at neuronerne i SNpr bliver overstimuleret, hvilket fører til excitotoksisk medieret neurodegeneration i SNpr. I studie III blev den inflammatoriske proces i forbindelse med excitotoksisk medieret neurodegeneration samt håndteringen af den øgede mængde af jern, som akkompagnerer den øgede infiltration af inflammatoriske celler, undersøgt. Studiet viste blandt andet, at både den neurodegenerative proces og den medførende inflammation var stærk og vedvarende i SNpr selv 91 dage, efter ibotensyre var blevet injiceret i striatum. I studie IV blev betydningen af kronisk neurodegeneration med inflammation derfor undersøgt i forhold til BBB permeabilitet og ændringer i genekspression af forskellige basalmembran og adhæsionsmolekyler. Ydermere, for at undersøge den cellulære respons af BBB på inflammation, blev en rotte BBB model bestående af BCECs, pericytter og astrocytter etableret og eksponeret for lipopolysaccharid (LPS).

Studiet viste tilstedeværelse af albumin immunoreaktion i SNpr, hvilket indikerer, at BBB havde været komprimeret i løbet af de 91 dage efter injektion af ibotensyre i striatum. Derudover var genekspressionen af *Icam1* og *Timp1* opreguleret i både modellen for neurodegeneration med inflammation og i BBB-modellen. I BBB-modellen blev den øgede ekspression af *Icam1* observeret i BCECs og astrocytterne, og den øgede ekspression af *Timp1* blev observeret i pericytten og astrocytten, hvilket indikerer, at disse celletyper bidrager til den øgede ekspression af *Icam1* og *Timp1* observeret *in vivo* som respons på excitotoksisk medieret neurodegeneration i SNpr.

ACKNOWLEDGEMENTS

First of all, I would like to thank my supervisor Professor Torben Moos, who has given me the opportunity to work as a Ph.D. student in his laboratory, *Laboratory of Neurobiology*. Torben Moos has besides being my supervisor for the last three years, also been the person, who introduced me to laboratory work on the 3rd semester of my bachelor degree. We created these amazing immunofluorescent pictures of different cell types of the brain and from that point on I knew that I wanted to be a scientist. Therefore, I would like to thank Torben Moos for inspiring me to take on the challenge and go for a career as a scientist, and for the valuable inputs and discussions during my Ph.D. study.

I would also like to thank everybody from the Laboratory of Neurobiology. Especially, Assistant Professor Louiza Bohn Thomsen, who is always ready to help whenever you need it, and Postdoc Annette Burkhart for teaching me how to isolate cells for the *in vitro* blood-brain barrier models, valuable discussions, and the many hours in the laboratory working side by side. I'm very grateful to you both for being such great colleagues, and also for being great travel mates and roommates whenever we have been out of town for conferences and seminars. Thanks to Lene Lundgaard Donovan for the (almost) endless discussions and troubleshooting when our RT-qPCR results suddenly didn't make any sense and Associate Professor Jacek Lichota for inputs to the gene expression analysis. Additionally, big thanks to the laboratory technicians Merete Fredsgaard, Hanne Krone Nielsen, and Ditte Bech for helping me out in laboratory, whenever I needed an extra hand.

I would, additionally, like to thank to Professor Svend Birkelund for great collaboration. Svend Birkelund is helpful and I appreciate the valuable feedback and troubleshooting advises he has giving me during my PhD study. Also thanks to Associate Professor Allan Stensballe for helping with the mass spectrometry analysis.

Furthermore, I would like to thank everybody in the Ph.D. office who all has made the long hours and everyday working environment so great. Also thanks to all my colleagues in the Biomedicine groups for great coffee-breaks and Associate Professor Meg Duroux for all our bike-talk, sometimes is good to talk about something else than work. A special thanks to fellow

Ph.D. student and friend Simone Riis who has always been ready to listening to complaints when things didn't go according to plan, or whenever I needed feedback on figures or a sentence.

Additionally, I would like to thanks Professor Warren Tate from the University of Otago with whom I wrote my master thesis. Warren was very inspiring and taught be a lot about how to present results and he also inspired me to take on the challenge and apply for a Ph.D. position.

Thanks to Fonden for Lægevidenskabens fremme, the Lundbeck foundation, and Aalborg University for financial support.

Last but not least, I would like to thank my friends and family for always supporting me. A special thanks to my partner Simon who has been a great support during the writing of this thesis.

Table of Contents

List of manuscripts.....	XIII
List of abbreviations	XIV
Chapter 1. The blood-brain barrier (BBB).....	17
1.1. The composition of the BBB.....	18
1.1.1. Brain capillary endothelial cells (BCECs)	18
1.1.2. Pericytes	21
1.1.3. Astrocytes.....	23
1.1.4. Vascular basement membrane.....	24
1.2. <i>In vitro</i> BBB models	26
Chapter 2. Neurodegeneration with inflammation	31
2.1. Microgliosis	31
2.2. Astrogliosis	32
2.3. Change of the BBB	34
2.3.1. Brain capillary endothelial cells (BCECs)	34
2.3.2. Pericytes	35
2.3.3. Astrocytes.....	36
2.3.4. Vascular basement membrane.....	36
Chapter 3. Thesis objectives.....	39
Chapter 4. Methods and Results.....	41
4.1. Study I.....	41
4.2. Study II.....	42
4.3. Study III	43
4.4. Study IV	44
Chapter 5. Discussion	45
5.1. Blood-brain barrier models	45
5.2. IgG transport across the BBB.....	47
5.3. Model of neurodegeneration with inflammation.....	47
5.4. Evaluation of blood-brain barrier permeability	48
Chapter 6. Conclusion and future perspectives.....	51
References.....	53
Appendix A. Study III	65

LIST OF MANUSCRIPTS

Study I:

Expression and deposition of basement membrane proteins by brain capillary endothelial cells in a murine model of the blood-brain barrier

Maj Schneider Thomsen, Svend Birkelund, Annette Burkhart, Allan Stensballe, Torben Moos

Manuscript in preparation

Study II:

Characterisation of the expression of the neonatal Fc receptor by murine brain capillary endothelial cells

Maj Schneider Thomsen, Svend Birkelund, Allan Stensballe, Torben Moos

Manuscript in preparation

Study III:

Neurodegeneration with inflammation is accompanied by accumulation of iron and ferritin in microglia and neurons

Maj Schneider Thomsen, Michelle Vandborg Andersen, Pia Rægaard

Christoffersen, Malene Duedal Jensen, Jacek Lichota, Torben Moos

Neurobiology of Disease (2015) 108-118

Study IV:

The neurovascular unit contributes to modulation in the expression of extracellular matrix proteins and adhesion molecules in an experimental model of neurodegeneration with inflammation

Maj Schneider Thomsen, Annette Burkhart, Torben Moos

Manuscript in preparation

Other activities:

Accessing Targeted Nanoparticles to the Brain: The Vascular Route

Annette Burkhart, Minaz Azizi, Maj Schneider Thomsen, Louiza Bohn Thomsen, Torben Moos

Current Medical Chemistry, 2014;21(36):4092-9

Targeted drug delivery to the brain using magnetic nanoparticles

Louiza Bohn Thomsen, Maj Schneider Thomsen, Torben Moos

Future medicine, 2015

Transfection of brain capillary endothelial cells in primary culture with defined blood-brain barrier properties

Annette Burkhart, Louiza Bohn Thomsen, Maj Schneider Thomsen, Jacek Lichota, Csilla Fazakas, Istcân Krizbai, Torben Moos

Fluids Barriers CNS 12:19. doi:10.1186/s12987-015-0015-9

LIST OF ABBREVIATIONS

A β	Amyloid beta
AJs	Adherence junctions
AMT	Adsorptive mediated transcytosis
Ang-1	Angiopoietin 1
AQP	Aquaporin
Ara-C	Cytosine beta-D-arabinofuranoside
α SMA	Alpha-smooth muscle actin
β 2m	Beta 2 microglobulin
BBB	Blood-brain barrier
BCECs	Brain capillary endothelial cells
bFGF	Basic fibroblast growth factor
BM	Basement membrane
CAA	Cerebral amyloid angiopathy
cAMP	Cyclic adenosine monophosphate
CNS	Central nervous system
CSF	Cerebrospinal fluid (CSF)
DAMP	Damage associated molecular pattern
EBM	Endothelial basement membrane
FBS	Fetal bovine serum
FcRn	Neonatal Fc receptor
GDNF	Glia cell-derived neurotrophic factor
GFAP	Glial fibrillary acidic protein
HSPG	Heparan sulphate proteoglycan
ICAM1	Intercellular Adhesion Molecule 1
IFN γ	Interferon gamma
IgG	Immunoglobulin G
IL	Interleukin
iNOS	Inducible nitric oxide synthase (iNOS)
JAM	Junctional adhesion molecule
LPS	Lipopolysaccharide
MAC1/CD11b	Macrophage antigen complex 1
mBCECs	Murine brain capillary endothelial cells
MCAO	Middle Cerebral Artery Occlusion
MIP	Macrophage inflammatory protein

MMP	Matrix metalloproteinase
NFκB	Nuclear factor kappa-light-chain-enhancer of activated B cells
NOX2	NADPH oxidase 2
NVU	Neurovascular unit
PAMP	Pathogen-associated molecular pattern
Papp	Apparent permeability coefficient
PBM	Parenchymal basement membrane
PDGFRβ	Platelet derived growth factor receptor beta
PDS	Plasma derived serum
Pgp	P-glycoprotein
PRR	Pattern recognition receptors
PVS	Perivascular space
RMT	Receptor mediated transcytosis
RNS	Reactive nitrogen species
ROS	Reactive oxygen species
SMC	Smooth muscle cells
SNpr	Substantia nigra pars reticulata
SPARC	Secreted protein acidic and rich in cysteine
TEER	Transendothelial electrical resistance
TfR	Transferrin receptor
TGFβ	Transforming growth factor
TIMP1	Tissue inhibitor of metalloproteinases
TJs	Tight junctions
TLR	Toll-like receptor
TNFα	Tumour necrosis factor alpha
VEGF	Vascular endothelial growth factor
ZO	Zonula occludens

Chapter 1. The blood-brain barrier (BBB)

The central nervous system (CNS) is protected from the circulation by two distinct barriers, i.e. the blood-brain barrier (BBB) and the blood-cerebrospinal fluid (CSF) barrier that both limit the penetration of toxins, pathogens, and many molecules into the brain (Abbott et al., 2006, Daneman et al., 2010a). The BBB is located at the brain microvasculature and denotes the major site of blood-CNS interchange (Mattsson et al., 2014). The BBB consists of thin non-fenestrated brain capillary endothelial cells (BCECs) connected by intermingling tight junctions (TJ) and adherence junctions (AJ). The BCECs are surrounded by pericytes embedded in the vascular basement membrane. The outer part of this basement membrane is further invested by astrocytic endfeet, and to some extent also projections from microglia, oligodendrocytes, and neurons. All together, these cells are referred to as the neurovascular unit (NVU) (Fig. 1) (Abbott et al., 2010).

Since the BBB restricts the entry of many molecules into the brain, the barrier also becomes an obstacle for the treatment of neurological disorders, as it also restricts the entry of many drugs. However, much research carried out in recent years acknowledges that the vascular integrity of the brain gets compromised in common neurological disorders like Alzheimer's disease (Biron et al., 2011, Zlokovic, 2011, Dorr et al., 2012), Parkinson's disease (Carvey et al., 2005, Patel et al., 2011), stroke (Fukuda et al., 2004), epilepsy (Marchi and Lerner-Natoli, 2012) and multiple sclerosis (Ortiz et al., 2014). Hypothetically, the pathological changes of the BBB in such neurological disorders may indirectly increase the success of drug delivery across the BBB.

The following paragraphs introduce the cellular compositions of the BBB and the associated basement membrane. Furthermore, the creation of *in vitro* BBB models is covered, including an introduction to some of the changes that can be observed at the BBB in neurological disorders with inflammation.

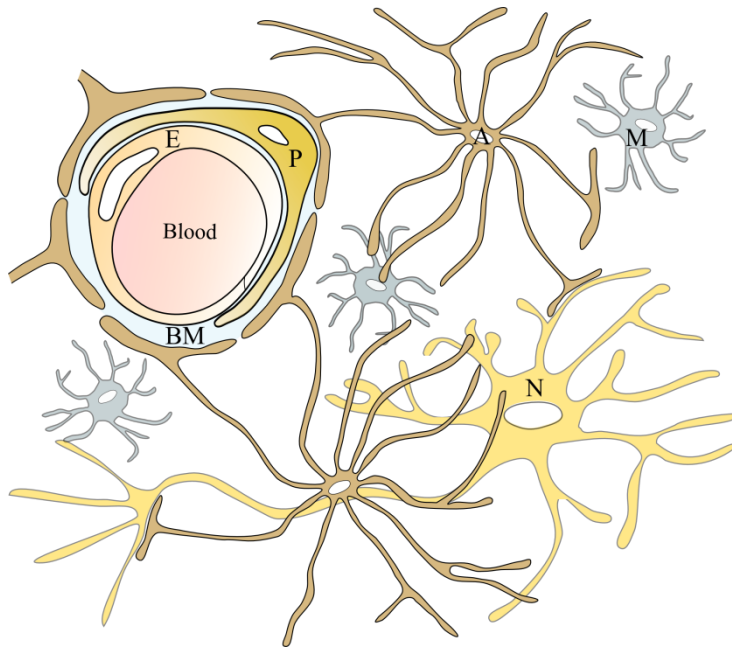


Figure 1. Schematic illustration of the neurovascular unit (NVU). The endothelial cell (E) lines the surface of the blood-vessel and is supported by the pericyte (P), which is embedded in the basement membrane (BM). The endothelial cells are further supported by astrocytic (A) endfeet and in close proximity are both the microglial (M) cells and neurons (N) located.

1.1. The composition of the BBB

1.1.1. Brain capillary endothelial cells (BCECs)

In brain capillaries, the BBB is primarily formed by BCECs, pericytes, and astrocytic endfeet. In larger vessels like arteries, arterioles and veins, the pericyte are replaced by smooth muscle cells. The BCECs are special compared to capillary endothelial cells in other parts of the body due to their tight interconnections made by TJs and AJs, their lack of fenestrations, and low vesicular transport. The AJs consist of different cadherins, which span the intercellular cleft. They are attached to the cytoplasm of the cells through catenins. The AJs are primarily responsible for holding the BCECs together, thereby giving structural support to the BCECs. The TJs are the primary component of the BBB that prominently restrict the paracellular transport across the BBB. The TJs consist of claudins and occludin, which span the

intercellular cleft and are linked to the cytoplasmic scaffolding proteins zonulae occludentes (ZO1-3) and cingulins. Furthermore, the junctional adhesion molecules (JAMs) also span the intercellular cleft and take part in the restriction of the paracellular transport (Wolburg et al., 2009, Abbott et al., 2010). The restriction in the free movement of ions across the BBB results in high *in vivo* transendothelial electrical resistance (TEER). The TEER in rat pial vessels was measured to $\sim 1500 \Omega \cdot \text{cm}^2$ (Butt et al., 1990). In frog microvessels an average of $1870 \Omega \cdot \text{cm}^2$ has been measured (Crone and Olesen, 1982). However, these measured values come nowhere near the calculated electrical resistance by Smith and Rapoport reporting a cerebrovascular permeability value of $8000 \Omega \cdot \text{cm}^2$ in the brain of rats (Smith and Rapoport, 1986).

The BCECs are the primary cell type responsible for ensuring the supply of essential nutrients into the brain (Fig. 2). O_2 , CO_2 , and small lipophilic agents can relatively freely cross the lipid membrane. However, the BCECs abundantly express ABC efflux transporters, which transport many crossing small lipophilic agents back to the blood. The ABC efflux transporters also restrict the entry of many toxins circulating in the blood. Few polar molecules, e.g. alcohols and morphine, can pass the BBB by paracellular diffusion through the TJs. Amino acids and glucose are transported across the BCECs via carrier mediated transport. This transport can be bi-directional, determined by the concentration gradient, or uni-directional, involving the exchange of one substance for another. Larger molecules like proteins are primarily transported through receptor mediated transcytosis (RMT) or adsorptive mediated transcytosis (AMT). Immune cells can also cross the BBB through a process called diapedesis. The immune cells enter the luminal side of the BCECs and before creating an opening at the abluminal side, the entry side is closed, thereby leaving the BBB intact. The immune cells can also cross the BBB paracellularly by modulation of the TJ proteins (Abbott et al., 2006, Abbott et al., 2010).

The special features of the BCECs are important for protecting and maintaining brain homeostasis although it also creates a major obstacle in the delivery of drugs to CNS. Therefore, several attempts are made in order to overcome the BBB. One approach is to target a transporter at the BBB, thereby using the BBBs own shuttle system to transport drugs across the BBB. One such target is the transferrin receptor (TfR). TfRs are expressed in many tissues, however, it is uniquely expressed at the luminal surface of the

capillaries of the brain (Jefferies et al., 1984), making the TfR a putatively perfect target for the delivery of drugs to the CNS. Bispecific antibodies targeting both the BCEC TfRs and a target in the diseased brain parenchyma are promising candidates for the treatment of brain disorders (Yu et al., 2011, Yu et al., 2014). However, the fate of the antibodies in the brain parenchyma is not well understood. The neonatal Fc receptor (FcRn) was proposed to be involved in the clearance of antibodies from brain to the blood (Deane et al., 2005, Cooper et al., 2013), and the design of tetravalent bispecific antibodies that both target the TfR, a brain target, and the FcRn were proposed to increase the pharmacological effect of the antibodies (Pardridge, 2015).

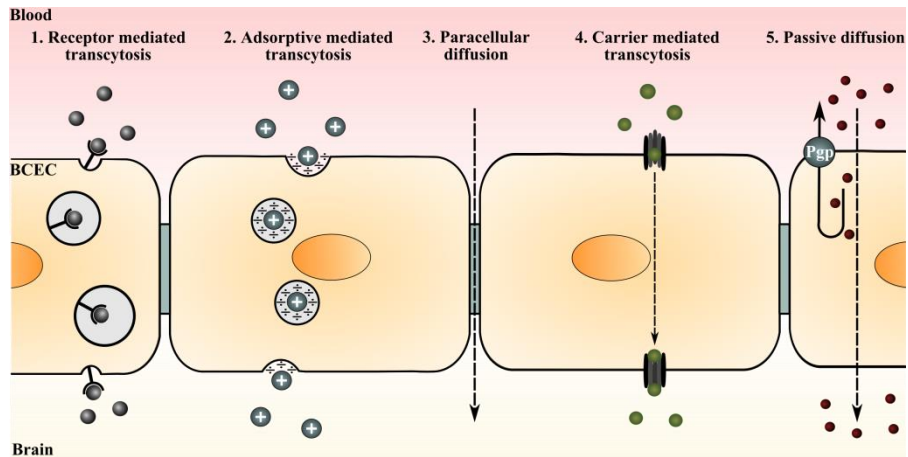


Figure 2. Schematic illustration of the different transport routes across the brain capillary endothelial cells (BCECs). Large proteins are primarily transported by either receptor mediated transcytosis (1) or adsorptive mediated transcytosis (2). A few small polar molecules, like alcohol, are able to cross the blood-brain barrier by paracellular diffusion (3) through the tight junctions. Glucose and amino acids can be transported across the BCECs by carrier mediated transcytosis (4). Small lipophilic agents can relatively freely cross the lipid membrane through passive diffusion (5). However, these are often transported back to the blood by ABC efflux transporters such as P-glycoprotein (Pgp) which are abundantly expressed by the BCECs. Adapted from (Abbott et al., 2006).

1.1.2. Pericytes

The continuous support of pericytes to the BCECs is essential for proper BBB function. Pericytes are polymorphic, elongated, multi-branched mural cells, which wrap around the BCECs of the microvasculature. The greater the number of pericytes the tighter is the vascular barrier (Shepro and Morel, 1993). It is estimated that the ratio of pericytes to endothelial cells in CNS is 1:1-1:3 and 1:10-1:100 in striated muscles (Shepro and Morel, 1993, Winkler et al., 2014). Pericytes are clearly involved in the formation and maintenance of the impermeability of the BBB during development. Furthermore, in functional pericytes deficient (platelet derived growth factor receptor beta (*Pdgfrb*^{-/-})) mice, an increased rate of transcytosis in BCECs has been observed (Daneman et al., 2010b). The increased transcytotic rate is partly modulated through expression of *Mfsd2a* in endothelial cells. Hence, *Mfsd2a*^{-/-} mice have a leaky BBB and show increased vesicular transcytosis. Looking at pericyte deficient mice, a positive correlation between *Mfsd2a* expression in the endothelial cells and the degree of pericyte coverage was found, which indicates that pericytes affect the vesicular traffic, through the modulation of *Mfsd2a* expression in BCECs (Ben-Zvi et al., 2014). In addition, increased capillary diameter, reduced vessel density, and increased permeability were observed in pericyte deficient mice (Armulik et al., 2010). A recent study demonstrates that the forkhead (*Foxf2*) transcription factor is specifically expressed in pericytes of the brain, and *Foxf2*^{-/-} knockout mice show vascular defects and failure to develop a normal BBB (Reyahi et al., 2015). This supports the finding from other studies using *Pdgfrb*^{-/-} mice as a model for pericyte deficiency.

The importance of pericytes for maintenance of the BBB is supported by *in vitro* studies as co-culturing BCECs with pericytes enhanced the TEER (Al Ahmad et al., 2009, Nakagawa et al., 2009, Daneman et al., 2010b, Shimizu et al., 2012). The increased tightness of the barrier was proposed to be modulated by pericyte secretion of transforming growth factor β 1 (TGF β -1) (Dohgu et al., 2005).

Currently, no individually specific marker has been identified for brain pericytes, as they share many markers with smooth muscle cells (SMC) located in the walls of arteries and arterioles, thereby leaving some observations on pericytes a controversy. Although they are not completely specific, some commonly accepted markers for brain pericytes include

alpha-smooth muscle actin (α -SMA), chondroitin sulfate proteoglycan NG2, PDGFR β , CD13, and desmin (Armulik et al., 2011).

Pericytes were suggested to be involved in the regulation of the cerebral blood flow, since the stimulation of mice whisker pads resulted in dilation of first order capillaries, before dilation of the penetrating arterioles (Hall et al., 2014). However, another study conclude that pericytes do not regulate blood-flow, since what is referred to as truly cerebral capillary pericytes do not contract *in vivo* (Hill et al., 2015). The opposing results of the two studies are probably due to different definition of pericytes, since no single marker for the identification of pericytes exists. A schematic illustration of the distribution of SMCs and pericytes are shown in figure 3.

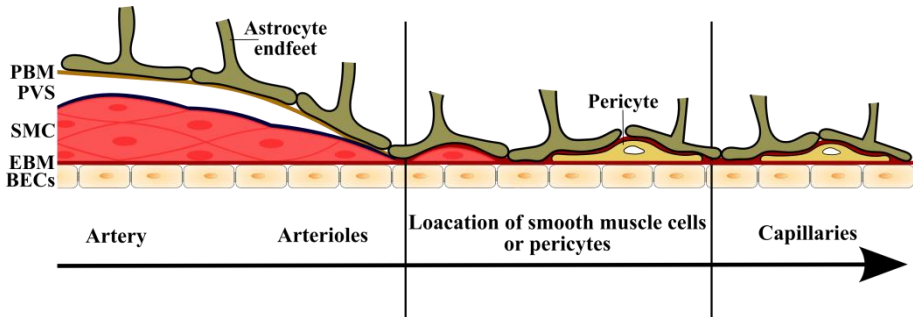


Figure 3. Distribution of smooth muscle cells (SMC) and pericytes in the vascular wall. Smooth muscle cells are present in the vessel wall in arteries and arterioles. At the pre-capillary level, both SMCs and pericytes are probably present but when reaching the capillaries it is only pericytes, which are present within the vessel wall. PBM: Parenchymal basement membrane, EBM: Endothelial basement membrane, BECs: Brain endothelial cells, PVS: Perivascular space.

Previously, α -SMA was used as a marker for pericyte differentiation, locating the α -SMA positive pericytes primarily in arterioles and venules and α -SMA negative pericytes in mid-capillaries (Hellstrom et al., 1999). The differentiation state of the pericytes is important for regulation of BBB integrity *in vitro*, since α -SMA negative pericytes are more prone to increase the TEER value compared to α -SMA positive pericytes (Thanabalasundaram et al., 2011, Tigges et al., 2012). TGF β is able to keep pericytes in their α -SMA positive state, whereas basic fibroblast growth factor (bFGF) maintains pericytes α -SMA negative (Thanabalasundaram et al., 2011). Pericytes lose the expression of α -SMA when grown in co-culture with astrocytes and/or BCECs, when the medium is supplemented with bFGF (Thomsen et al.,

2015a). These results indicate that pericytes might be able to change both phenotype, from α -SMA positive to α -SMA negative, and function depending on their stimulation at the BBB *in vivo*.

Increasing evidence also suggests that pericytes can transform into multipotent stem cells (Dore-Duffy et al., 2006, Nakagomi et al., 2015). Capillary pericytes grown in serum-free medium display changed morphology, when growing as non-adherent spheres that express nestin and NG2. These spheres could differentiate to cells expressing either marker of astrocytes, oligodendrocytes, or neurons primarily in combination with the expression of α -SMA (Dore-Duffy et al., 2006).

It is obvious that the overall potential of these peculiar pericytes has not yet been fully elucidated. There is no doubt that pericytes are important for the function of the BBB; however, the involvement of pericytic stem cells in the brain and their regulation of blood flow are less clear.

1.1.3. Astrocytes

Astrocytes are star-shaped glial cells with multiple functions in the CNS. They provide physical and metabolic support for neurons, and they are crucial for the maintenance of many BBB functions. When grown in co-culture with BCECs, astrocytes increase the TEER, which has been related to communicative secretion to the BCECs (Gaillard et al., 2001, Patabendige and Abbott, 2014, Burkhart et al., 2015). Hence, astrocytes can induce TJs partly through the secretion of sonic hedge hock, (Wang et al., 2014). Glia cell-derived neurotrophic factor (GDNF) also secreted from astrocytes contributes to increased TEER and reduced permeability of BCECs (Igarashi et al., 1999). Astrocytes also secrete TGF β 1, which upregulates the expression of TJ proteins (Merwin et al., 1990, Garcia et al., 2004) and increase the expression of the efflux transporter P-glycoprotein (Pgp) in BCECs of the fetal and neonatal brain (Baello et al., 2014). Angiopoietin 1 (Ang-1) and bFGF are also produced by astrocytes and take part in the induction of TJ proteins (Lee et al., 2003).

The astrocytic endfeet, which circumvent the basement membrane of the BBB (Fig. 1), have a high expression density of the water channel aquaporin 4 (AQP4) and the K⁺ channel Kir4.1. The expression of AQP4 and Kir4.1 is regulated by the interaction of astrocytic α -dystroglycan with the basement membrane protein agrin (Noell et al., 2011). The coupling with agrin

provides evidence that the basement membrane of the BBB is important for the interaction between cells of the BBB.

1.1.4. Vascular basement membrane

The vascular basement membrane denotes a specialised extracellular matrix 20-200 nm thick. It consists of a three dimensional network composed of proteins from four major glycoprotein families, i.e. laminins, collagen IV isoforms, nidogens, and heparan sulphate proteoglycans (HSPG) (Timpl, 1989, Engelhardt and Sorokin, 2009). In addition, the vascular basement membrane is also composed of minor components like secreted protein acidic and rich in cysteine (SPARC), fibulin 1 and 2, fibronectin, collagen types VIII, XV, XVIII, and thrombospondins 1 and 2 (Hallmann et al., 2005). The basement membrane is generated by self-assembly by both laminins and collagen IV into polymer networks, which are linked together through the binding of nidogens and the HSPGs perlecan. Laminin is also the primary component connecting the basement membrane to the surrounding structures (Yurchenco and Schittny, 1990, Hallmann et al., 2005, Roberts et al., 2012).

In CNS large blood vessels the basement membrane consists of two principally different entities, an endothelial and a parenchymal basement membrane, which can be distinguished by their composition of laminin. Hence, the endothelial basement membrane contains laminin $\alpha 4$ and $\alpha 5$, whereas the parenchymal basement membrane contains laminin $\alpha 1$ and $\alpha 2$. In large vessels penetrating the brain surface, the endothelial and parenchymal basement membranes are separated by a perivascular space, whereas in smaller blood vessels there is no clear separation between the endothelial and parenchymal basement membranes. Thus, the basement membrane of small vessels appears as a single basement membrane entity and contains both endothelial cell laminins $\alpha 4$ and $\alpha 5$, and laminin $\alpha 2$ produced by astrocytes, but no laminin $\alpha 1$ as in larger vessels (Sixt et al., 2001, Hallmann et al., 2005).

The basement membrane is very important for integration of BCECs and other cells of the NVU. Endothelial cells and astrocytes have several receptors for basement membrane proteins that act to anchor the cells to their respective basement membranes, hence contributing to stability of the BBB (Engelhardt and Sorokin, 2009). The basement membrane displays a high

capacity for binding of soluble factors such as vascular endothelial growth factor (VEGF) and bFGF (Bashkin et al., 1989, Hallmann et al., 2005). Thus, the basement membrane is likely to contribute to barrier function.

In addition, the individual components of the basement membrane have different functions. Laminins are cross-shaped and consist of an α -chain in combination with both a β -chain and γ -chain. Five α , four β , and three γ chains have been identified and these are able to combine and form 18 different laminin isoforms. The different laminin isoforms are named by their chain composition. The biological role of the laminins is largely defined through their interaction of the α -chain with cell surface receptors (Yousif et al., 2013). The laminins of the vascular basement membrane consist of either $\alpha 1$, $\alpha 2$, $\alpha 4$ or $\alpha 5$ in combination with $\beta 1$ and $\gamma 1$ chains composing the following laminin isoforms 111, 211, 411, and 511 (Hallmann et al., 2005). The importance of different laminin isoforms in the brain was supported by the creation of different laminin knockout mice models. Deletion of astrocytic laminin $\alpha 2$ cause bleeding in deep regions of the murine brain, whereas deletion of endothelial laminin $\alpha 4$ reduce the migration of T cells across the BBB in a mouse model of multiple sclerosis. Thus, laminins are important for both maintenance of the BBB and for defining sites for extravasation of inflammatory cells (Wu et al., 2009, Sorokin, 2010, Chen et al., 2013).

Collagen IV of the vascular basement membrane is a threadlike molecule derived from three polypeptide chains [$\alpha 1(IV)_2\alpha 2(IV)$] (Yurchenco and Schittny, 1990). In collagen IV [$\alpha 1(IV)_2\alpha 2(IV)$] knockout mice, collagen IV proved unnecessary for the deposition of basement membrane components during early embryonic development. However, the deletion caused embryonic lethality due to an impaired stability of the basement membrane at later embryonic age (Poschl et al., 2004).

The heparan sulfate proteoglycan perlecan has a multi-domain protein core and three glycosaminoglycan chains at its N-terminus. Perlecan is integrated in the collagen IV/laminin network and important for the maintenance of the basement membrane integrity and binding of growth factors (Gohring et al., 1998, Roberts et al., 2012). The binding of growth factors is primarily through the glycosaminoglycan chains, and perlecan is thereby able to modulate the paracrine signalling of the surrounding cells (Whitelock et al., 2008). Fibronectin forms a dimer of two almost identical

units involved in attachment of cells to other cells or the basement membrane (Tilling et al., 1998).

In vitro, the basement membrane is also important for barrier properties. By growing porcine BCECs on filters coated with either laminin, collagen IV, fibronectin or a mixture of one-to-one of these proteins, the TEER was significantly increased. The greatest increase in TEER was observed when the BCECs were grown on collagen IV, collagen IV/fibronectin, and fibronectin/laminin coated inserts (Tilling et al., 1998).

1.2. *In vitro* BBB models

In vitro BBB models have become a valuable tool for the study of the cellular interaction at the BBB as outlined in the previous sections, but also for investigations of the cellular response of the BBB to different insults. The *in vitro* system allows for mechanistic investigations of the BBB, which would otherwise have been virtually impossible to perform *in vivo* (Ogunshola, 2011).

The *in vitro* BBB models only resemble the *in vivo* properties of the BBB to some extent. Thus, a thorough characterisation is important before investigating any specific responses of the BBB. The BCECs are characterised by the complex interconnection through TJs. The *in vitro* BCECs should therefore express these complex TJ proteins and have restricted paracellular diffusion. The paracellular pathway can be assessed through the measure of TEER and the apparent permeability coefficient (Papp) for different molecules (Reichel et al., 2003).

Various *in vitro* BBB models have been developed constituting BCECs isolated from human (Siddharthan et al., 2007), porcine ((Patabendige and Abbott, 2014, Thomsen et al., 2015a), bovine (Helms and Brodin, 2014), rat (Nakagawa et al., 2009, Burkhart et al., 2015), and murine brains (Coisne et al., 2005, Shayan et al., 2011).

Both primary cell cultures and immortalised cell lines have been used to construct the *in vitro* BBB models. The immortalised cell cultures have been established after isolation of the endothelial cells, e.g. by conditionally immortalisation by introducing the temperature-sensitive simian virus 40 large T-antigen (Siddharthan et al., 2007). The immortalised cell lines are frequently used due to their ease compared to primary cells, which can be difficult to isolate, reveals a low yield, and their isolation can be complicated

by contamination by other cell types (Ogunshola, 2011). Some of the most widely used immortalised brain endothelial cell lines include the Rat Brain Endothelial Cell line RBE4, the human brain microvessel endothelial cell line hBMEC/D3, and the murine brain endothelial cell line b.End3. However, a great disadvantage of using immortalised cell lines is that they tend to lose many of their *in vivo* characteristics like restricted paracellular diffusion when grown in culture for multiple passages (Reichel et al., 2003). Thus, primary cells will resemble the *in vivo* situation more, and the results obtained from culture of primary cells are more likely to replicate the *in vivo* situation.

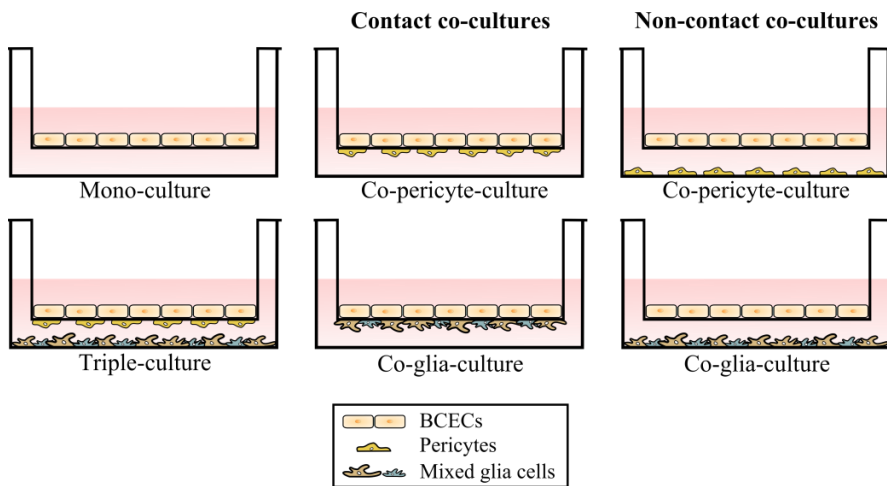


Figure 4. Illustration of different *in vitro* blood-brain barrier (BBB) models using the Transwell system. The brain capillary endothelial cells (BCECs) are grown on top of the porous filter membranes. The BCECs can be grown in contact or non-contact co-culture with either pericytes or mixed glial cells. The model which resembles the BBB *in vivo* the most is denoted by the triple-culture consisting of BCECs grown on the top of the inserts, pericytes on the back, and mixed glial cells in the bottom of the wells.

One of the largest challenges in the isolation of BCEC is the contamination of pericytes. BCECs express the efflux transporter Pgp, and are able to survive relative high concentrations of the Pgp substrate puromycin. Therefore, treatment of isolated BCECs with puromycin, greatly reduces the amount of pericytes (Perriere et al., 2005, Calabria et al., 2006). To further enhance the purity of the BCECs, substitution of fetal bovine

serum (FBS) with bovine platelet-poor plasma-derived serum (PDS) greatly improves BCEC culture purity. The effect of PDS is correlated to the lack of platelet-derived growth factor in PDS, which stimulates growth of pericytes and smooth muscle cells (Gordon et al., 1991, Calabria et al., 2006).

The Transwell system is the most commonly used system for the construction of *in vitro* BBB models (Fig. 4). The BCECs are seeded in inserts containing a porous filter membrane, which allows for the formation of a monolayer and induction of cell polarity. Pericytes or astrocytes are subsequently seeded on the back of the filters hence creating either a contact co-culture or in the bottom of the wells creating a non-contact co-culture. The model, which reassembles the BBB *in vivo* the most, is denoted by the triple-culture that contains BCECs, pericytes, and astrocytes (Ogunshola, 2011).

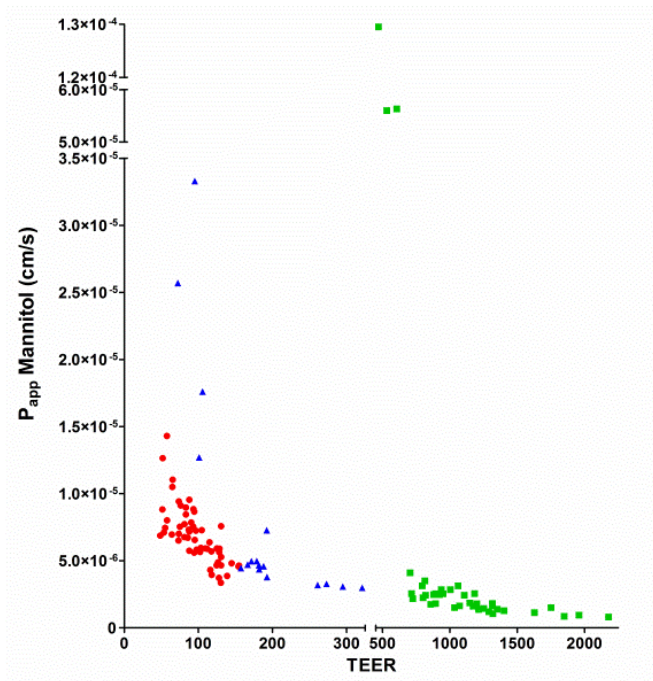


Figure 5. Graphical illustration of the apparent permeability coefficient (P_{app}) to mannitol in three different *in vitro* models. P_{app} is plotted against the measured Transendothelial electrical resistance (TEER) for murine (red), rat (blue) and porcine (green) brain capillary endothelial cells. The data are provided with acceptance from Study I, Burkhart et al. (2015), and Thomsen et al. (2015).

Besides co-culturing the cells of the BBB, the addition of soluble factors are beneficial for induction of barrier properties. Increased levels of intracellular cyclic adenosine monophosphate (cAMP) increase the TEER. This can be obtained by the addition of a combination of a cAMP analogue (CPT-cAMP) and a phosphodiesterase inhibitor (Ro 20-1724) (Rubin et al., 1991, Rist et al., 1997). The increased cAMP level cause increased phosphorylation of claudin-5 which leads to increased claudin-5 at the contact points between BCECs, thereby contributing to the increase in TEER (Soma et al., 2004). Like increased levels of cAMP, the addition of physiological levels of hydrocortisone (550 nM) also increases TEER (Hoheisel et al., 1998, Forster et al., 2005).

TEER varies greatly among the species from where the BCECs are isolated. Rat BCECs usually have higher TEER than their murine counterpart (Shayan et al., 2011, Burkhardt et al., 2015), and the TEER obtained by BCECs from both porcine and bovine are much higher than those obtained from rodents (Helms and Brodin, 2014, Patabendige and Abbott, 2014, Thomsen et al., 2015a). Although higher TEER values persist in porcine and bovine models, there are good indications that the rodent models do not need TEER values of that magnitude to obtain a similar low permeability to mannitol. To obtain a Papp for mannitol below $5 \cdot 10^{-6}$ cm/s, the TEER for rat BCECs should be above $\sim 150 \Omega \cdot \text{cm}^2$ (Burkhardt et al., 2015), for porcine BCECs above $\sim 600 \Omega \cdot \text{cm}^2$ (Thomsen et al., 2015a), and murine BCECs above $\sim 130 \Omega \cdot \text{cm}^2$ (Study I) (Fig. 5).

Chapter 2. Neurodegeneration with inflammation

As outlined in the previous sections the complex interaction between the BCECs, pericytes, astrocytes, and the basement membrane is crucial for proper BBB function. Conditions with neurodegeneration like Alzheimer's disease, Parkinson's disease and multiple sclerosis are accompanied by inflammation and perturbation of the BBB (Jansson et al., 2014, Monson et al., 2014). Some of the characteristic features associated with inflammation in CNS include activation of microglia cells and astrocytes (reactive gliosis) with a subsequent release of various inflammatory mediators that lead to changes of the brain microenvironment associated with increased permeability of the BBB and migration of inflammatory cells into the CNS (Vivekanantham et al., 2015).

2.1. Microgliosis

Microglial cells are resident macrophages of the CNS that act as the first line of defence to brain insults (Alliot et al., 1999, Rezai-Zadeh et al., 2009). Microglia expresses different pattern recognition receptors (PRRs) through which they detect changes of the brain microenvironment. The receptors recognise pathogen-associated molecular pattern (PAMPs) from microorganisms or damage-associated molecular patterns (DAMPs), which are endogenous components released by stressed, dying, or dead neurons. These receptors include Toll-like receptors (TLRs), RIG-1 like receptors, Nod-like receptors, and macrophage antigen complex 1 (MAC1/CD11b) the latter also functioning as an adhesion molecule (Chen et al., 2015).

Compared to resting microglia that have small cell bodies and thin ramified processes, activated microglial cells change morphology exhibiting enlarged cell body and irregular shape (Qin et al., 2013). The activated microglia release various pro-inflammatory mediators like cytokines, prostaglandins, chemokines, reactive oxygen species (ROS), and reactive nitrogen species (RNS), which amplify the inflammatory response, and exacerbate the neurodegeneration (Chen et al., 2015). Lipopolysaccharide (LPS) activates microglia cells through the interaction with CD11b, which leads to increased expression of NADPH-oxidase 2 (NOX2) and

subsequently increased production of ROS (Fig. 6). The increased production of ROS is correlated to the maintenance of the neuroinflammatory process (Pei et al., 2007, Qin et al., 2013). The pro-inflammatory cytokines released by activated microglia cells also include tumour necrosis factor alpha (TNF- α) and different isoforms of interleukin-1 (IL-1 β , IL-1 α). *In vitro* BCECs have increased permeability to sodium-fluorescein in response to microglia produced TNF- α , thereby correlating the production of TNF α to BBB dysfunction (Nishioku et al., 2010). α -synuclein binding to TLR4 on microglia cells results in translocation of nuclear factor kappa-light-chain-enhancer of activated B cells (NF- κ B) to the nucleus and subsequently expression and secretion of TNF α , IL-6 and CXCL1 (Fellner et al., 2013). Furthermore, the production of IL-1 by microglial cells are correlated with astrocyte proliferation (Giulian et al., 1986). Activated microglia also secrete a wide variety of chemokines involved in the cellular migration and communication (Tambuyzer et al., 2009).

2.2. Astrogliosis

Astrocytes are important for maintaining brain homeostasis e.g. through the support of the BBB function and regulation of the extracellular balance of ions and neurotransmitters. Reactive astrogliosis refers to the process whereby astrocytes become activated in response to different insults of the CNS such as neurodegeneration, infections, and trauma (Sofroniew, 2009). The activated astrocytes have hypertrophic cellular processes and increased expression of intermediate filaments, including glial fibrillary acidic protein (GFAP) (Pekny and Nilsson, 2005). The response of the activated astrocytes depends on the underlying cause varying from beneficial to harmful (Zamanian et al., 2012, Sofroniew, 2015). In severe astrogliosis, the astrocytes can proliferate and form a scar on the border between the healthy and damaged brain tissue (Fig. 6) (Sofroniew, 2009).

Astrocytes are important for maintaining a low extracellular level of glutamate and blockage of the astrocyte glutamate transports GLAST and GLT-1 leads to increased extracellular glutamate levels and subsequent excitotoxicity induced neurodegeneration (Rothstein et al., 1996). Thus, it has been proposed that reactive astrogliosis are valuable for not intensifying excitotoxic-induced neurodegeneration (Sofroniew, 2009).

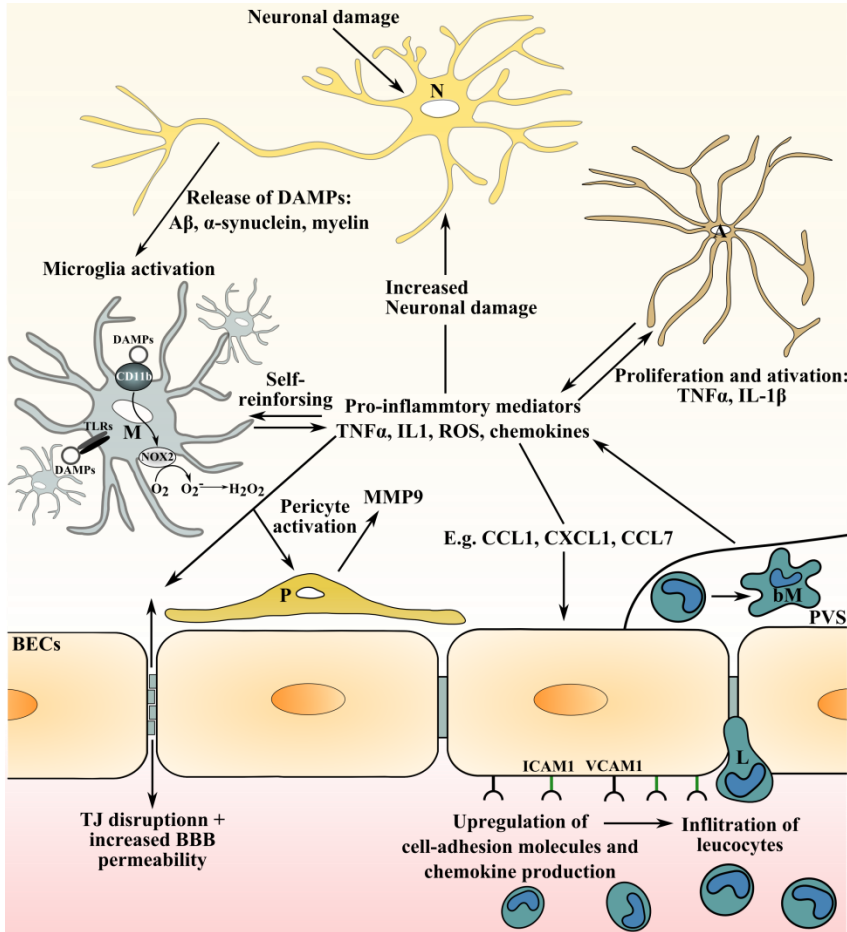


Figure 6. Simplified illustration of the cellular response to neurodegeneration. Various insults can lead to neuronal (N) damage causing the release of damage-associated molecular patterns (DAMPs). The DAMPs activates the microglial cells (M) through binding to the pattern recognition receptors such as toll-like receptor (TLR) and CD11b. The microglial cells then release various cytokines, chemokines, and reactive oxygen species (ROS), which contributes to neuronal damage and activate surrounding cells, such as the pericyte (P), astrocytes (A) and brain endothelial cells (BECs). The endothelial cells upregulate their expression of cell adhesion molecules such as vascular cell adhesion molecule 1 (VCAM1) and intercellular adhesion molecule 1 (ICAM1) and release chemokines, which leads to the infiltration of leucocytes (L). The infiltrating leucocytes differentiate in the perivascular space (PVS) to brain macrophages (bM), which contribute to the neuroinflammatory process.

In vitro studies using primary cultures reveal that astrocytes in response to common pro-inflammatory cytokines (TNF α , IL-1 β) secrete chemokines like CCL2, CCL7, and CXCL1 (Thompson and Van Eldik, 2009, Fellner et al., 2013). These results were confirmed *in vivo* where intrahippocampal injection of TNF α or IL-1 β increased the production of CCL2 and CXCL1 in the astrocytes. This increased production of chemokines in the inflamed brain lead to recruitment of inflammatory cells to the brain parenchyma from the periphery (Thompson and Van Eldik, 2009). After *in vitro* LPS exposure, astrocytes also secrete pro-inflammatory cytokines, such as IL-1 β , TNF- α , and IL-6 which can aggravate the inflammatory response (Li et al., 2015).

2.3. Change of the BBB

2.3.1. Brain capillary endothelial cells (BCECs)

As a response to chronic neurodegeneration with inflammation the BCECs have changed permeability. Increased permeability to the plasma protein-binding dye Evans Blue and increased deposition of major plasma proteins like immunoglobulin G (IgG) and fibrinogen were observed in brains of transgenic mouse models of Alzheimer's disease (Dickstein et al., 2006, Paul et al., 2007, Ryu and McLarnon, 2009, Biron et al., 2011, Merlini et al., 2011). Other major features related to changes in the vascular integrity in Alzheimer's disease are increased capillary density due to neoangiogenesis (Patel et al., 2011), hypervascularity (Biron et al., 2011), and disruption of tight junctions between BCECs (Marco and Skaper, 2006, Liu et al., 2011). Identical changes are seen in multiple sclerosis in where an altered expression of tight junction and adherence junction proteins are observed in the lesion areas in conjunction with astrogliosis and leakage of serum proteins (Kirk et al., 2003, Alvarez et al., 2011). Also, in Parkinson's disease, increased permeability of the BBB has been observed (Sarkar et al., 2014).

Some of the changes observed in such distinct diseases are possibly related to the common underlying neuroinflammation associated to the neurodegeneration. The BCECs respond to the increased production of cytokines and chemokines by increasing the expression of cell-adhesion molecules thereby promoting the infiltration of leucocytes to the brain (Fig. 6), which is believed to contribute to the neuroinflammation and BBB

changes (Brown et al., 1994, Sorokin, 2010, Larochelle et al., 2011). The primary site for leucocyte trafficking into the brain is at the post-capillary venules (Sorokin, 2010).

In brain regions with neurodegeneration and inflammation an increase deposition of iron is also observed (Connor et al., 1992, Bartzokis et al., 1999, LeVine et al., 2013). The increase in iron load is proposed to relate to infiltration of iron-containing leucocytes in particularly monocytes. The monocytes transform to brain macrophages, engulfing cellular debris, and when they die out, their iron-content is released, which further contributes to neurodegeneration and production of ROS (Andersen et al., 2014).

2.3.2. Pericytes

Pericytes are important for development and maintenance of the BBB. The embedding inside the basement membrane makes the pericyte an obvious player in brain inflammation. Like other cells of the brain, the pericytes are able to synthesise chemokines such as CCL2, CXCL9, and CXCL10 and in response to pro-inflammatory stimuli with LPS or cytokines like TNF α , IL-1 β and interferon gamma (IFN γ) (Jansson et al., 2014). The stimulation of pericytes with TNF α also leads to increased production of MMP9 and the cytokines macrophage inflammatory protein (MIP)-1 α and IL-6 (Takata et al., 2011, Matsumoto et al., 2014). TNF α stimulated pericytes are also strong activators of microglia cells, which increase their expression of IL-1 β and inducible nitric oxide synthase (iNOS) adding to the inflammatory process (Matsumoto et al., 2014). In a mouse model of multiple sclerosis, pericytes change their expression of integrins, hence promoting the proliferation and migration of pericytes. An identical change in integrin expression is observed, when pericytes are stimulated with TNF α *in vitro* (Tigges et al., 2013).

Brain vessels of Alzheimer's disease mice have decreased pericyte coverage compared to the wild type, and the remaining pericytes have elongated and hypertrophic processes (Park et al., 2013). Congruent to observations in Tg2576 mice, the number of pericytes in autopsies from Alzheimer patients are decreased, and their surface coverage of brain capillaries reduced (Baloyannis and Baloyannis, 2012, Sengillo et al., 2013). Morphologically, the remaining pericytes exhibit increased number of pinocytotic vesicles, large lipid granules, and mitochondrial alterations,

suggesting, that their functionality is compromised (Baloyannis and Baloyannis, 2012). Furthermore, a tight correlation between reduced pericyte coverage and extravascular IgG and fibrin deposition have been observed in Alzheimer's disease subjects (Sengillo et al., 2013), which strongly supports the notion of pericytes being important for maintaining the integrity of the BBB. It should not be overlooked, however, that opposing results were reported. Hence, investigations on post mortem brain samples from Alzheimer's and Parkinson's patients revealed no difference in degenerative pericytes compared to control specimens (Farkas et al., 2000).

2.3.3. Astrocytes

The support of the astrocytic endfeet is important for maintaining the functions of the BBB. Thus, retraction of the endfeet can cause impairment of the BBB and lead to increased permeability. Retraction of astrocyte endfeet has been observed in a mouse model of Alzheimer's disease especially in brain areas affected by cerebral amyloid angiopathy (CAA) (Merlini et al., 2011). CAA is a condition where amyloid β ($A\beta$) are being deposited in the vessel wall and is correlated to approximately 80 % of Alzheimer's disease cases (Deane and Zlokovic, 2007). In addition, a major hallmark in Alzheimer's disease is the formation of intracellular neurofibrillary tangles, which are composed of hyperphosphorylated tau protein. The cerebral response to injected mutant tauP301L in mice after 10 and 21 days is the presence of swollen astrocyte endfeet and increased thickening of the capillary vessel walls (Jaworski et al., 2011). Also, in a mouse model of multiple sclerosis retraction of astrocytes endfeet has been observed. The retraction was correlated to a decreased expression of β dystroglycan which is involved in attachment of the endfeet to the vasculature through the interaction with vascular laminin (Agrawal et al., 2006). Retraction of astrocyte endfeet is also observed, in post-mortem brain specimens from patients with multiple sclerosis (Claudio et al., 1995).

2.3.4. Vascular basement membrane

As previously described, the basement membrane is important for proper function of the BBB, and changes of the basement membrane are observed in response to neurodegeneration with inflammation. To some extent this is related to the release of cytokines and proteases by invading inflammatory

cells. The secretion of matrix metalloproteinases (MMPs) is correlated to the remodelling of the basement membrane, and the resulting cleaved protein fragments are believed to affect both activity and function of infiltrating and resident cells (Sorokin, 2010).

MMPs belong to a family of calcium dependent and zinc containing endopeptidases. They are produced in a latent form and contain multiple regions including a N-terminal signal peptide, a propeptide responsible for maintaining MMP in a latent state and C-terminal hemopexin-like domain. The latter is essential for the recognition of MMPs by the tissue inhibitor of metalloproteinases (TIMPs). Different enzymes or free radicals can activate MMPs through direct cleavage of the prodomain or by a cysteine switch mechanism (Brkic et al., 2015). The function of MMPs is regulated on multiple levels. Increased MMP transcription is seen in response to proinflammatory cytokines, and then MMP can be activated by removal of the prodomain, or inhibited by TIMP recognition (Loffek et al., 2011).

In Alzheimer's disease, three distinct changes in the basement membrane are seen, i.e. deposition of amyloid beta ($A\beta$) in the vessel wall also referred to as CAA, basement membrane thickening, and changes in the protein composition (Deane and Zlokovic, 2007). The cause of the $A\beta$ deposition in the vessel wall remains unknown, but it is linked to both a decreased clearance of $A\beta$ across the BBB and thickening of the basement membrane (Okoye and Watanabe, 1982, Deane and Zlokovic, 2007). Basement membrane thickening is observed in the capillaries of Alzheimer's disease patients (Mancardi et al., 1980, Zarow et al., 1997, Farkas et al., 2000). The cause of the basement membrane thickening is not fully elaborated just like the fact that the cell-types responsible for its thickening are unknown. Astrocytes are suggested to be mainly responsible for the thickening, since immune electron microscopy revealed that only the parenchymal basement membrane was affected (Zarow et al., 1997). Basement membrane thickening is also seen in post mortem brain samples from Parkinson's disease patients (Farkas et al., 2000), and in multiple sclerosis increased deposition of fibrin and collagen are seen in post mortem specimens (Claudio et al., 1995).

The distribution of individual basement membrane proteins is altered in Alzheimer's disease. The amount of collagen IV and laminin decrease and the amount of fibronectin and perlecan conversely increase in brains of an aged Alzheimer's mouse model (Hawkes et al., 2013). The changes in

basement membrane composition could accelerate the accumulation of A β , since perlecan accelerates A β fibril formation and stabilise newly formed fibrils (Castillo et al., 1997). The pericyte is also linked to the changes in the basement membrane composition observed in Alzheimer's disease. Human pericytes cultured in the presence of A β increase their concentration of both mRNA and protein concentration of agrin and glypican-1 (Timmer et al., 2009). Increased soluble agrin has also been observed in the vasculature in human autopsies of late stage Alzheimer's disease, where it associates with A β -plaques and the vascular basement membrane (Berzin et al., 2000).

Chapter 3. Thesis objectives

The complex interaction of the components of NVU are of outermost importance for proper function of the BBB, and hence also for maintaining a healthy brain microenvironment. The objective of the thesis has therefore been to obtain a more thorough understanding of the BBB in health and disease, using an *in vitro* murine BBB model, and an *in vivo* model for chronic neurodegeneration.

For the investigation of the overall objective of the thesis, four separate experimental studies have been generated each with separate aims. Study I and II are related to the normal BBB using a murine *in vitro* BBB model, whereas consequences of neurodegeneration with inflammation are investigated in study III and IV in a rat model of neurodegeneration with inflammation.

Study I: To establish and characterise four different murine *in vitro* BBB models using primary murine brain capillary endothelial cells (mBCECs), pericytes and mixed glial cells. Furthermore, the contribution of the mBCECs to the synthesis of basement membrane proteins is investigated.

Study II: To investigate the expression of the neonatal Fc Receptor (FcRn) in the *in vitro* BBB model with mBCECs grown in co-culture with mixed glial cells established in study I.

Study III: To investigate inflammatory response and the handling of iron in an experimental *in vivo* model of neurodegeneration with inflammation.

Study IV: To investigate the state of the BBB in the same experimental *in vivo* model of neurodegeneration with inflammation as established in study III.

Chapter 4. Methods and Results

4.1. Study I

Expression and deposition of basement membrane proteins by brain capillary endothelial cells in a primary murine model of the blood-brain barrier

Maj Schneider Thomsen, Svend Birkelund, Annette Burkhart, Allan Stensballe and Torben Moos

Manuscript in preparation

Abstract

Background: Many cerebral conditions with neurodegeneration, e.g. Alzheimer's disease, Parkinson's disease and multiple sclerosis are accompanied by inflammation and changes in the vascular basement membrane. The changes of the basement membrane are thought to contribute to structural changes of the blood-brain barrier (BBB). Primary cell models of the cerebral vasculature are valuable tools for studying various insults to the BBB. The aim of the present study has been to characterise four different *in vitro* setups of the murine BBB and investigate the expression of basement membrane proteins by the murine brain capillary endothelial cells (mBCECs).

Methods: Primary mBCECs and pericytes were isolated from adult mouse brains. Mixed glial cells (mainly astrocytes and microglia) were prepared from cerebral cortices of newborn mice. The mBCECs were grown in four setups: in mono-culture, and in co-culture with pericytes, mixed glial cells, or both. The integrity of the BBB models was evaluated by measures of transendothelial electrical resistance (TEER) and passive permeability to mannitol. To study the expression of basement membrane proteins RT-qPCR, mass spectrometry and immunofluorescent labelling were used.

Results: The four different murine BBB model setups were developed and characterised. Co-culturing of mBCECs with pericytes, mixed glial cells, or both significantly increased the TEER compared to the mono-culture, and a low passive permeability was correlated with high TEER. The mBCECs were found to express major basement membrane proteins *in vitro* and the expression of laminin $\alpha 5$ and collagen IV $\alpha 1$ was regulated by the culture conditions.

Conclusion: Here we present a model of the murine BBB with defined BBB properties: high TEER, low permeability to mannitol and expression of endothelial markers (claudin-5 and ZO1). Furthermore, the obtained data reveal that mBCECs synthesise major basement proteins *in vitro*.

4.2. Study II

Characterisation of the expression of the neonatal Fc receptor by murine brain capillary endothelial cells

Maj Schneider Thomsen, Svend Birkelund, Allan Stensballe, Torben Moos

Manuscript in preparation

Abstract

Background: The neonatal Fc receptor (FcRn) is presumed to be involved in the clearance of antibodies from the brain parenchyma to the blood and this mechanism can be an important function for immunotherapy delivery to the brain. The usage of *in vitro* blood-brain barrier (BBB) models has become a valuable tool for the study of various functions of the BBB, such as protein transport and the response of the BBB to different stimuli. The aim of the present study was, therefore, to characterise a murine *in vitro* BBB model for the expression of FcRn.

Methods: Primary cultures of murine brain capillary endothelial cells (mBCECs) were grown in co-culture with mixed glial cells and analysed for the expression of FcRn using a polyclonal (M-255) and a monoclonal (1G3) antibody.

Results and conclusions: The immunolabeling with M-255 and 1G3 of mBCECs *in vitro* was negative, however, after additional analysis it was concluded that FcRn is indeed expressed albeit at low levels by the mBCECs as determined with RT-qPCR and mass spectrometry. Furthermore, transfection with mouse FcRn of mBCECs showed detectable amount of FcRn in the cytoplasm.

4.3. Study III

Neurodegeneration with inflammation is accompanied by accumulation of iron in microglia and neurons

Maj Schneider Thomsen, Michelle Vandborg Andersen, Pia Rægaard Christoffersen, Malene Duedal Jensen, Jacek Lichota, Torben Moos

Published in *Neurobiology of Disease*, Volume 81, September 2015, Pages 108-118

The manuscript can be seen in appendix A.

Abstract

Chronic inflammation in the substantia nigra (SN) accompanies conditions with progressive neurodegeneration. This inflammatory process contributes to gradual iron deposition that may catalyze formation of free-radical mediated damage, hence exacerbating the neurodegeneration. This study examined proteins related to iron-storage (ferritin) and iron-export (ferroportin) (aka metal transporter protein 1, MTP1) in a model of neurodegeneration. Ibotenic acid injected stereotactically into the striatum leads to loss of GABAergic neurons projecting to SN pars reticulata (SNpr), which subsequently leads to excitotoxicity in the SNpr as neurons here become vulnerable to their additional glutamatergic projections from the subthalamic nucleus. This imbalance between glutamate and GABA eventually led to progressive shrinkage of the SNpr and neuronal loss. Neuronal cell death was accompanied by chronic inflammation as revealed by the presence of cells expressing ED1 and CD11b in the SNpr and the adjacent white matter mainly denoted by the crus cerebri. The SNpr also exhibited changes in iron metabolism seen as a marked accumulation of inflammatory cells containing ferric iron and ferritin with morphology corresponding to macrophages and microglia. Ferritin was detected in neurons of the lesioned SNpr in contrast to the non-injected side. Compared to non-injected rats, surviving neurons of the SNpr expressed ferroportin at unchanged level. Analyses of dissected SNpr using RT-qPCR showed a rise in ferritin-H and -L transcripts with increasing age but no change was observed in the lesioned side compared to the non-lesioned side, indicating that the increased expression of ferritin in the lesioned side occurred at the post-transcriptional level. Hpcidin transcripts were higher in the lesioned side in contrast to ferroportin mRNA that remained unaltered. The continuous entry of iron-containing inflammatory cells into the degenerating SNpr and their subsequent demise is probably responsible for iron donation in neurodegeneration. This is accompanied by only a slight increase in neuronal ferritin and not ferroportin, which suggests that the iron-containing debris of dying inflammatory cells and degenerating neurons gets scavenged by invading macrophages and activated microglia to prevent an increase in neuronal iron.

4.4. Study IV

The neurovascular unit contributes to modulation in the expression of extracellular matrix proteins and adhesion molecules in an experimental model of neurodegeneration with inflammation

Maj Schneider Thomsen, Annette Burkhart Larsen, Torben Moos

Manuscript in preparation

Abstract

Introduction: The blood-brain barrier (BBB) represents the interface between the blood and brain parenchyma, and is important for ensuring sufficient nutrient transport and for maintaining brain homeostasis. Many conditions with neurodegeneration and inflammation are accompanied by changes of the BBB, including increased BBB permeability and changes of the vascular basement membrane. We have previously in an experimental model of neurodegeneration shown that excitotoxic-induced neurodegeneration in substantia nigra pars reticulata (SNpr) was accompanied by activation of microglial cells and infiltration of inflammatory cells. We therefore aimed to investigate if the neurodegeneration with inflammation is associated with changes of the BBB.

Method: The model of neurodegeneration with inflammation was created by stereotactical injection of ibotenic acid into the striatum, which subsequently results in excitotoxicity in SNpr. We examined the BBB permeability by immunolabeling of endogenous albumin, and injection of green fluorescent liposomes. The changes of the basement membrane and adhesion molecules were investigated using a PCR array for 84 different genes. Subsequently, nine of these genes were chosen for additional RT-qPCR analysis (*Fnl*, *Col6a1*, *Col8a1*, *Spp1*, *Ctgf*, *Icam1*, *Cdh1*, *Mmp3*, *Timp1*). To further investigate the response of BBB to inflammation, an *in vitro* BBB model containing primary rat brain capillary endothelial cells (rBCECs), pericytes and astrocytes was exposed to lipopolysaccharide (LPS) and investigated for the expression of most of the genes analysed in the *in vivo* model.

Results/conclusion: Our findings indicate that in response to the neurodegeneration with inflammation increased BBB permeability and changes in the expression of the basement membrane protein collagen IV can be observed. Also a large increase in *Icam1* and *Timp1* are observed both in the model of neurodegeneration with inflammation and *in vitro* in response to the exposure to LPS. *In vitro* the increased expression of *Icam1* was seen in rBCECs and astrocytes, and increased expression of TIMP1 was seen in pericytes and astrocytes suggesting that these cells are at least partly responsible for the increased expression of *Icam1* and *Timp1* seen *in vivo* in response to excitotoxic-induced neuronal death in SNpr.

Chapter 5. Discussion

The first part (study I and II) of this thesis was related to the BBB in normal physiological conditions. The main objective of study I was to establish a model of the murine BBB using primary mBCECs, pericytes, and mixed glial cells, and to investigate the contribution of the mBCECs to the synthesis of basement membrane proteins. Four types of BBB models were created consisting of mBCECs grown in mono-culture, in co-culture with pericytes, or mixed glial cells, and in triple-culture with both pericytes and mixed glial cells. Using the co-culture model with mBCECs and mixed glial cells established in study I, the expression of the FcRn was investigated in study II.

The second part of the thesis (study III and IV) investigated the consequences of chronic neurodegeneration with inflammation. In study III, the inflammatory response and handling of iron were investigated in a rat model with neurodegeneration caused by excitotoxicity in SNpr. Using the same model, the state of the BBB and gene expression of basement membrane and adhesion molecules were investigated in study IV.

5.1. Blood-brain barrier models

In study I, four different murine *in vitro* BBB setups were established and characterised. The mBCECs and pericytes were successfully isolated from the brains of 6 to 10 weeks old mice. The mBCECs were identified by immunolabeling of the tight junction proteins claudin-5 and ZO1. Furthermore, high purity of the mBCEC cultures was obtained by growing the isolated cells in specialised growth medium with puromycin. The mBCECs have high expression of the efflux transporter Pgp. Thus, they are able to survive relative high amounts of puromycin (Perriere et al., 2005, Calabria et al., 2006).

The differentiation state of the pericytes is important for their capabilities of inducing BBB integrity (Thanabalasundaram et al., 2011, Yao et al., 2014). The pericytes were identified by immunolabeling of α -SMA and PDGFR β . The pericyte culture contained pericytes, which were both α -SMA and PDGFR β positive, and pericytes with a more disorganised staining pattern with only a weak expression α -SMA (from now referred to as α -

SMA negative). The isolated pericytes were grown in basic growth medium until confluent, where they were passaged to filters and the medium changed to mBCEC medium with bFGF. After 4 days, the mBCECs were seeded on top of the filters. The pericytes were therefore immunolabeled after they had been grown 4 days in medium with bFGF. The addition of bFGF has been proposed to maintain the pericytes in an α -SMA negative state, which is the main type of pericytes responsible for the induction of barrier properties (Thanabalasundaram et al., 2011). The pericytes were equally as potent as the mixed glial cell culture to induce high TEER of the mBCECs, which indicates that the pericyte culture contained a sufficient amount of α -SMA negative pericytes. The pericytes could also change phenotype during the co-culturing with mBCECs, since it was previously shown that porcine pericytes lose their α -SMA expression after co-culturing with porcine BCECs (Thomsen et al., 2015a).

The mixed glial cells were isolated from brain cortices of new-born mice. The culture contained primarily astrocytes and some microglial cells identified by immunolabeling of GFAP and CD11b, respectively. The microglial cells grow on top of the astrocytes (Schildge et al., 2013), and to diminish the amount of microglia the cultures were vigorously washed in PBS. For the induction of BBB properties, the presence of microglia cells and possible oligodendrocytes are acceptable, since these cell types are also in close proximity to the BBB *in vivo*. However, when specific functions of astrocytes are investigated, the presence of other glial cells can become an obstacle. Therefore, to obtain enriched astrocyte cultures different approaches exist. Shaking of the of the culture on an orbital shaker or adding of the antimetabolic toxin cytosine β -D-arabinofuranoside (Ara-C) and the lysosomotropic agent L-leucine methyl ester are methods, which have been developed to obtain enriched astrocytes cultures (Hamby et al., 2006, Schildge et al., 2013).

In the present study, a murine BBB model was developed since most genetic modified animal are mice. Thus, for the investigation of genetic modified mouse models the construction of a murine BBB model are of great value for future investigations of conditions that would otherwise have been virtually impossible to study *in vivo*. However, it should also be noted that the yield of BCECs isolated from mouse brain are less than the yield from both rat and porcine brains, based on the experience from our lab.

Thus, the creation of primary murine BBB models is more costly than those models created of BCECs isolated from rat and porcine brains.

5.2. IgG transport across the BBB

Data indicates that the FcRn are involved in the clearance of the off IgG from brain to the blood (Deane et al., 2005, Cooper et al., 2013). In the search for new treatment strategies for treatment of neurodegenerative diseases, much research have been carried out in order to develop bispecific antibodies, which are able to bind both to the TfR, whereby the antibodies can be shuttled across the BBB, while simultaneously binding or neutralising a target of the diseased brain tissue (Yu et al., 2011, Yu et al., 2014). To further increase the pharmacological effect of the antibodies, the design of tetravalent bispecific antibodies which targets the TfR, a brain target, and FcRn has been proposed (Pardridge, 2015). The initial purpose of study II was therefore to investigate the involvement of FcRn IgG transport across mBCECs *in vitro*. This was, however, complicated by problems in identifying the receptor. This is a good example of the importance of proper characterisation of the model before initiation of the investigations (Reichel et al., 2003). The expression of FcRn in mBCECs was confirmed with RT-qPCR and mass spectrometry and immunolabeling of mouse brain tissue. However, we only observed immunolabeling of FcRn in few capillary structures, which questions the biological relevance of designing tetravalent bispecific antibodies (Pardridge, 2015). Thus, the involvement of FcRn in the efflux of IgG still remains a dispute.

5.3. Model of neurodegeneration with inflammation

In study III and IV, a model of neurodegeneration with inflammation was created by stereotactic injection of the glutamate receptor agonist ibotenic acid into striatum, leading to cell death among the GABAergic neurons projecting to substantia nigra pars reticulata (SNpr). Subsequently, this results in an overstimulation of the neurons in SNpr from the glutamate projections from nucleus subthalamicus (Sastry and Arendash, 1995). Glutamate is a major excitatory neurotransmitter in the CNS, and the imbalance between glutamate and GABA will therefore eventually result in neurodegeneration in SNpr caused by excitotoxicity. The neurodegeneration and accompanying neuroinflammation is thereby being created at a remote

site from the initial injection site. The relevance of creating a model with excitotoxic-induced neurodegeneration is supported by the fact that conditions with chronic neurodegeneration such as Parkinson's disease and Alzheimer's disease also are accompanied by glutamate mediated neurotoxicity (Mehta et al., 2013). The glutamate mediated neurotoxicity is believed to be mediated through two processes. The first part cause acute swelling of the cell body and peripheral processes through opening of cation channels followed by a slowly evolving degeneration of the neurons, possibly mediated by the influx of Ca^{2+} (Koh and Choi, 1991, Hynd et al., 2004).

In study IV the *in vivo* studies were supported by *in vitro* investigations of the response of the BBB to stimulation with LPS. LPS is a major part of the wall of gram-negative bacteria, and it can be used to create an inflammatory response both *in vivo* and *in vitro*. LPS was added to the bottom chamber, and the cells were exposed to LPS for 17 hours as previously described (Coisne et al., 2005). In response to LPS, the TEER significantly decreased compared to the control cells. The decrease in TEER was not accompanied by significant change in claudin-5 expression. This is supported by another study investigating the *in vitro* response of the BBB to LPS. Immunolabeling of claudin-5 revealed no change in organisation oppositely, to both organisation of ZO1 and occludin which was altered in response to LPS exposure (Banks et al., 2015). This indicates that the decreased TEER could be a result of changed expression of ZO1 and occludin, and not claudin-5.

5.4. Evaluation of blood-brain barrier permeability

In study IV, the immunolabeling of albumin on post-surgery day 91 revealed large patches of immunoreaction in the lesioned side and no immunoreaction in the non-lesioned side. This indicates that the BBB has been compromised during the 91 days post-surgery. To evaluate BBB permeability on post-surgery day 28 and 91, 75 nm green fluorescent liposomes were injected two hours prior to the termination of the rats. No apparent permeability was observed and the detection of the green fluorescent liposomes was complicated by autofluorescence within the brain tissue.

BCECs are non-fenestrated, thus, the transcellular permeability is low and only small lipophilic molecules <1nm in size are able to pass through the

BCECs (Sarin, 2010). However, the transcellular passaging is further complicated by the expression of efflux transporters by the BCECs, which transport crossing molecules back to the blood (Abbott et al., 2010). Furthermore, the BCECs have low paracellular transport due to the complex interaction of the TJ proteins (Wolburg et al., 2009, Abbott et al., 2010). Increased paracellular permeability can be caused by changes in the TJ proteins, whereby small intercellular gaps are created, allowing the passage across the BBB of plasma proteins such as albumin and infiltration of leucocytes (Stamatovic et al., 2008). The interaction and distribution of the TJ proteins are affected by their phosphorylation state (Kago et al., 2006, Stamatovic et al., 2006).

Depending on the underlying pathology, different factors are involved in the changed permeability of the BBB. As shown in both the study III and IV, the neurodegeneration caused by excitotoxicity in SNpr was accompanied by activation of microglia, astrocytes and infiltration of inflammatory cells. Thus, the alteration of the BBB is possible related to the inflammatory response to the neurodegeneration. The activated glial cells and infiltrating inflammatory cells secrete multiple pro-inflammatory mediators (Fig. 6), which can affect the permeability of the BBB (Thompson and Van Eldik, 2009, Nishioku et al., 2010, Fellner et al., 2013).

Different approaches exist to evaluate BBB permeability. Liu et al. (2015) investigated the BBB permeability in three different mouse models (Middle Cerebral Artery Occlusion (MCAO), LPS, and cold injury) by injection of Evans blue (Liu et al., 2015). Evans blue has high affinity for albumin and can be visualised by excitation with a laser. Thus, basically detection of Evans blue equals the detection of albumin (Radu and Chernoff, 2013). The greatest leakage was observed after MCAO and was accompanied by decrease expression of claudin-5 and VE-cadherin. Banks et al. (2015) also investigated the BBB permeability after LPS induced inflammation. For the measure of BBB permeability, ^{14}C -sucrose and radioactive labelled albumin was injected. Subsequently radioactivity was measured in plasma and in the brain (Banks et al., 2015). Both these studies detect BBB permeability by investigating albumin distribution to the brain. Albumin (67 kDa) is ~7nm (Sarin, 2010), therefore, the injection of 75 nm green fluorescent liposomes might be too large to move across the BBB even by paracellular diffusion in the case of disruption of TJ proteins.

Recently, Bien-Ly et al. (2015) investigated the BBB permeability in four different mouse models of Alzheimer's disease and in a mouse model of multiple sclerosis. In the model of multiple sclerosis, both increased passage of injected antibodies, extravasated IgG, and albumin was observed. This was contrasted in the different mouse models of Alzheimer's disease in where no change in permeability was observed compared to control animals to any of the injected radioiodinated molecules (3 kDa dextran, 67 kDa albumin, and 150 kDa IgG) or different antibodies. However, when the mice were treated with LPS 6 hours prior to termination, a significant increase in BBB passage of 3 kDa dextran was observed. Furthermore, when post-mortem brains of Alzheimer's disease patients were compared with control samples, no differences were observed in the amount of plasma proteins leakage in micro infarcts. Increased leakage would indicate areas with impaired BBB (Bien-Ly et al., 2015). The results of the study by Bien-Ly et al. (2015) is thereby questioning the general belief that increased BBB permeability is present in both Alzheimer's disease patients and mouse models of Alzheimer's disease and that this could contribute to disease progression and increase delivery of therapeutics. However, it should still be noted that multiple studies report increased Evans blue extravasation and increased deposition of major plasma proteins like IgG, and fibrinogen in brains of other transgenic mouse models of Alzheimer's disease and in post mortem samples from Alzheimer's disease patients (Dickstein et al., 2006, Paul et al., 2007, Ryu and McLarnon, 2009, Biron et al., 2011, Merlini et al., 2011). These contradicting results underline the great diversity existing between different animal models and the actual pathology of the disease seen in humans, and certainly open for more investigations.

Chapter 6. Conclusion and future perspectives

Study I. Four different experimental setups of the murine BBB were successfully established and characterised. The mBCECs express major basement membraneproteins *in vitro*, and the expressions of laminin $\alpha 5$ and collagen IV $\alpha 1$ were regulated by the culture conditions. For future studies, the contribution of the pericytes and astrocytes to the synthesis of basement membrane proteins would give valuable information about the basement membrane composition. However, before initiation of such experiments, an enriched astrocyte culture with few contaminating microglia cells would be needed. This also applies for the pericyte culture, in which microglial cells consistently were observed at varying degrees between isolations.

Study II. The mBCECs had low expression of the FcRn. Future studies should include investigations on the beta-2 microglobulin ($\beta 2m$) expression by the mBCECs, since $\beta 2m$ is important for the function of FcRn. Moreover, more evaluations are needed on whether the expression of recombinant FcRn reflects *de facto* transport of IgG.

Study III. “The neurodegenerative insult induced by excitotoxicity led to inflammation and accumulation of iron-containing microglia in the SNpr. The microglia probably act to scavenge excess iron originating from degrading neurons, glia and invading ferritin- and ED1- immunoreactive macrophages, but when their capacity is exceeded iron accumulates in the neurons as evinced from the larger content of neuronal ferritin. In contrast, no change in ferroportin expression was observed, which could be the result of counteracting regulation of its expression, i.e., increased post-transcriptionally expression via its regulation by IRE and a decreased post-translational expression via interaction with hepcidin at the cellular membrane“ (Thomsen et al., 2015b).

Study IV. The neurodegeneration induced by excitotoxicity was accompanied by increased BBB permeability as evaluated by the presence of endogenous albumin within the brain parenchyma. No apparent permeability was observed by injection of 75 nm green fluorescent liposomes 2 hours

prior to termination on post-surgery day 28 and 91. In future studies I would investigate the tempo-spatial aspect of the BBB permeability, and the size dependency by injection of different molecules with a size variation up until 75 nm. Increased expression of *Icam1* and *Timp1* was also observed. *In vitro* the increased expression of *Icam1* was seen in rBCECs and astrocytes, and increased expression of *Timp1* was seen in pericytes and astrocytes suggesting that these cells are, at least partly, responsible for the increased expression of *Icam1* and *Timp1* seen *in vivo*. Therefore to evaluate if the increased expression of *Icam1* and *Timp1* distributes to the identical cell types *in vivo* immunolabeling is needed. Furthermore, to quantify the expression of basement membrane proteins *in vivo*, I would support the gene expression analyses with Western blot analyses.

REFERENCES

- Abbott, N. J., Patabendige, A. A., Dolman, D. E., Yusof, S. R. & Begley, D. J. 2010. Structure and function of the blood-brain barrier. *Neurobiol Dis*, 37, 1, 13-25.
- Abbott, N. J., Ronnback, L. & Hansson, E. 2006. Astrocyte-endothelial interactions at the blood-brain barrier. *Nat Rev Neurosci*, 7, 1, 41-53.
- Agrawal, S., Anderson, P., Durbeej, M., Van Rooijen, N., Ivars, F., Opdenakker, G. & Sorokin, L. M. 2006. Dystroglycan is selectively cleaved at the parenchymal basement membrane at sites of leukocyte extravasation in experimental autoimmune encephalomyelitis. *J Exp Med*, 203, 4, 1007-19.
- Al Ahmad, A., Gassmann, M. & Ogunshola, O. O. 2009. Maintaining blood-brain barrier integrity: pericytes perform better than astrocytes during prolonged oxygen deprivation. *J Cell Physiol*, 218, 3, 612-22.
- Alliot, F., Godin, I. & Pessac, B. 1999. Microglia derive from progenitors, originating from the yolk sac, and which proliferate in the brain. *Brain Res Dev Brain Res*, 117, 2, 145-52.
- Alvarez, J. I., Cayrol, R. & Prat, A. 2011. Disruption of central nervous system barriers in multiple sclerosis. *Biochim Biophys Acta*, 1812, 2, 252-64.
- Andersen, H. H., Johnsen, K. B. & Moos, T. 2014. Iron deposits in the chronically inflamed central nervous system and contributes to neurodegeneration. *Cell Mol Life Sci*, 71, 9, 1607-22.
- Armulik, A., Genove, G. & Betsholtz, C. 2011. Pericytes: developmental, physiological, and pathological perspectives, problems, and promises. *Dev Cell*, 21, 2, 193-215.
- Armulik, A., Genove, G., Mae, M., Nisancioglu, M. H., Wallgard, E., Niaudet, C., He, L., Norlin, J., Lindblom, P., Strittmatter, K., Johansson, B. R. & Betsholtz, C. 2010. Pericytes regulate the blood-brain barrier. *Nature*, 468, 7323, 557-61.
- Baello, S., Iqbal, M., Bloise, E., Javam, M., Gibb, W. & Matthews, S. G. 2014. TGF-beta1 regulation of multidrug resistance P-glycoprotein in the developing male blood-brain barrier. *Endocrinology*, 155, 2, 475-84.
- Baloyannis, S. J. & Baloyannis, I. S. 2012. The vascular factor in Alzheimer's disease: a study in Golgi technique and electron microscopy. *J Neurol Sci*, 322, 1-2, 117-21.
- Banks, W. A., Gray, A. M., Erickson, M. A., Salameh, T. S., Damodarasamy, M., Sheibani, N., Meabon, J. S., Wing, E. E., Morofuji, Y., Cook, D. G. & Reed, M. J. 2015. Lipopolysaccharide-induced blood-brain barrier disruption: roles of cyclooxygenase, oxidative stress, neuroinflammation, and elements of the neurovascular unit. *J Neuroinflammation*, 12, 1, 223.
- Bartzokis, G., Cummings, J. L., Markham, C. H., Marmarelis, P. Z., Treciokas, L. J., Tishler, T. A., Marder, S. R. & Mintz, J. 1999. MRI evaluation of brain iron in earlier- and later-onset Parkinson's disease and normal subjects. *Magn Reson Imaging*, 17, 2, 213-22.

- Bashkin, P., Doctrow, S., Klagsbrun, M., Svahn, C. M., Folkman, J. & Vlodavsky, I. 1989. Basic fibroblast growth factor binds to subendothelial extracellular matrix and is released by heparitinase and heparin-like molecules. *Biochemistry*, 28, 4, 1737-43.
- Ben-Zvi, A., Lacoste, B., Kur, E., Andreone, B. J., Mayshar, Y., Yan, H. & Gu, C. 2014. Mfsd2a is critical for the formation and function of the blood-brain barrier. *Nature*, 509, 7501, 507-11.
- Berzin, T. M., Zipser, B. D., Rafii, M. S., Kuo-Leblanc, V., Yancopoulos, G. D., Glass, D. J., Fallon, J. R. & Stopa, E. G. 2000. Agrin and microvascular damage in Alzheimer's disease. *Neurobiol Aging*, 21, 2, 349-55.
- Bien-Ly, N., Boswell, C. A., Jeet, S., Beach, T. G., Hoyte, K., Luk, W., Shihadeh, V., Ulufatu, S., Foreman, O., Lu, Y., Devoss, J., Van Der Brug, M. & Watts, R. J. 2015. Lack of Widespread BBB Disruption in Alzheimer's Disease Models: Focus on Therapeutic Antibodies. *Neuron*, 88, 2, 289-97.
- Biron, K. E., Dickstein, D. L., Gopaul, R. & Jefferies, W. A. 2011. Amyloid triggers extensive cerebral angiogenesis causing blood brain barrier permeability and hypervascularity in Alzheimer's disease. *PLoS One*, 6, 8, e23789.
- Brkic, M., Balusu, S., Libert, C. & Vandenbroucke, R. E. 2015. Friends or Foes: Matrix Metalloproteinases and Their Multifaceted Roles in Neurodegenerative Diseases. *Mediators Inflamm*, 2015, 620581.
- Brown, Z., Gerritsen, M. E., Carley, W. W., Strieter, R. M., Kunkel, S. L. & Westwick, J. 1994. Chemokine gene expression and secretion by cytokine-activated human microvascular endothelial cells. Differential regulation of monocyte chemoattractant protein-1 and interleukin-8 in response to interferon-gamma. *Am J Pathol*, 145, 4, 913-21.
- Burkhart, A., Thomsen, L. B., Thomsen, M. S., Lichota, J., Fazakas, C., Krizbai, I. & Moos, T. 2015. Transfection of brain capillary endothelial cells in primary culture with defined blood-brain barrier properties. *Fluids Barriers CNS*, 12, 19.
- Butt, A. M., Jones, H. C. & Abbott, N. J. 1990. Electrical resistance across the blood-brain barrier in anaesthetized rats: a developmental study. *J Physiol*, 429, 47-62.
- Calabria, A. R., Weidenfeller, C., Jones, A. R., De Vries, H. E. & Shusta, E. V. 2006. Puromycin-purified rat brain microvascular endothelial cell cultures exhibit improved barrier properties in response to glucocorticoid induction. *J Neurochem*, 97, 4, 922-33.
- Carvey, P. M., Zhao, C. H., Hende, B., Lum, H., Trachtenberg, J., Desai, B. S., Snyder, J., Zhu, Y. G. & Ling, Z. D. 2005. 6-Hydroxydopamine-induced alterations in blood-brain barrier permeability. *Eur J Neurosci*, 22, 5, 1158-68.
- Castillo, G. M., Ngo, C., Cummings, J., Wight, T. N. & Snow, A. D. 1997. Perlecan binds to the beta-amyloid proteins (A beta) of Alzheimer's disease, accelerates A beta fibril formation, and maintains A beta fibril stability. *J Neurochem*, 69, 6, 2452-65.

References

- Chen, S. H., Oyarzabal, E. A. & Hong, J. S. 2015. Critical role of the Mac1/NOX2 pathway in mediating reactive microglia-generated chronic neuroinflammation and progressive neurodegeneration. *Curr Opin Pharmacol*, 26, 54-60.
- Chen, Z. L., Yao, Y., Norris, E. H., Krueyer, A., Jno-Charles, O., Akhmerov, A. & Strickland, S. 2013. Ablation of astrocytic laminin impairs vascular smooth muscle cell function and leads to hemorrhagic stroke. *J Cell Biol*, 202, 2, 381-95.
- Claudio, L., Raine, C. S. & Brosnan, C. F. 1995. Evidence of persistent blood-brain barrier abnormalities in chronic-progressive multiple sclerosis. *Acta Neuropathol*, 90, 3, 228-38.
- Coisne, C., Dehouck, L., Faveeuw, C., Delplace, Y., Miller, F., Landry, C., Morissette, C., Fenart, L., Cecchelli, R., Tremblay, P. & Dehouck, B. 2005. Mouse syngenic in vitro blood-brain barrier model: a new tool to examine inflammatory events in cerebral endothelium. *Lab Invest*, 85, 6, 734-46.
- Connor, J. R., Menzies, S. L., St Martin, S. M. & Mufson, E. J. 1992. A histochemical study of iron, transferrin, and ferritin in Alzheimer's diseased brains. *J Neurosci Res*, 31, 1, 75-83.
- Cooper, P. R., Ciambone, G. J., Kliwinski, C. M., Maze, E., Johnson, L., Li, Q., Feng, Y. & Hornby, P. J. 2013. Efflux of monoclonal antibodies from rat brain by neonatal Fc receptor, FcRn. *Brain Res*, 1534, 13-21.
- Crone, C. & Olesen, S. P. 1982. Electrical resistance of brain microvascular endothelium. *Brain Res*, 241, 1, 49-55.
- Daneman, R., Zhou, L., Agalliu, D., Cahoy, J. D., Kaushal, A. & Barres, B. A. 2010a. The mouse blood-brain barrier transcriptome: a new resource for understanding the development and function of brain endothelial cells. *PLoS One*, 5, 10, e13741.
- Daneman, R., Zhou, L., Kebede, A. A. & Barres, B. A. 2010b. Pericytes are required for blood-brain barrier integrity during embryogenesis. *Nature*, 468, 7323, 562-6.
- Deane, R., Sagare, A., Hamm, K., Parisi, M., Larue, B., Guo, H., Wu, Z., Holtzman, D. M. & Zlokovic, B. V. 2005. IgG-assisted age-dependent clearance of Alzheimer's amyloid beta peptide by the blood-brain barrier neonatal Fc receptor. *J Neurosci*, 25, 50, 11495-503.
- Deane, R. & Zlokovic, B. V. 2007. Role of the blood-brain barrier in the pathogenesis of Alzheimer's disease. *Curr Alzheimer Res*, 4, 2, 191-7.
- Dickstein, D. L., Biron, K. E., Ujiie, M., Pfeifer, C. G., Jeffries, A. R. & Jefferies, W. A. 2006. A beta peptide immunization restores blood-brain barrier integrity in Alzheimer disease. *FASEB J*, 20, 3, 426-33.
- Dohgu, S., Takata, F., Yamauchi, A., Nakagawa, S., Egawa, T., Naito, M., Tsuruo, T., Sawada, Y., Niwa, M. & Kataoka, Y. 2005. Brain pericytes contribute to the induction and up-regulation of blood-brain barrier functions through transforming growth factor-beta production. *Brain Res*, 1038, 2, 208-15.
- Dore-Duffy, P., Katychev, A., Wang, X. & Van Buren, E. 2006. CNS microvascular pericytes exhibit multipotential stem cell activity. *J Cereb Blood Flow Metab*, 26, 5, 613-24.

- Dorr, A., Sahota, B., Chinta, L. V., Brown, M. E., Lai, A. Y., Ma, K., Hawkes, C. A., McLaurin, J. & Stefanovic, B. 2012. Amyloid-beta-dependent compromise of microvascular structure and function in a model of Alzheimer's disease. *Brain*, 135, Pt 10, 3039-50.
- Engelhardt, B. & Sorokin, L. 2009. The blood-brain and the blood-cerebrospinal fluid barriers: function and dysfunction. *Semin Immunopathol*, 31, 4, 497-511.
- Farkas, E., De Jong, G. I., De Vos, R. A., Jansen Steur, E. N. & Luiten, P. G. 2000. Pathological features of cerebral cortical capillaries are doubled in Alzheimer's disease and Parkinson's disease. *Acta Neuropathol*, 100, 4, 395-402.
- Fellner, L., Irschick, R., Schanda, K., Reindl, M., Klimaschewski, L., Poewe, W., Wenning, G. K. & Stefanova, N. 2013. Toll-like receptor 4 is required for alpha-synuclein dependent activation of microglia and astroglia. *Glia*, 61, 3, 349-60.
- Forster, C., Silwedel, C., Golenhofen, N., Burek, M., Kietz, S., Mankertz, J. & Drenckhahn, D. 2005. Occludin as direct target for glucocorticoid-induced improvement of blood-brain barrier properties in a murine in vitro system. *J Physiol*, 565, Pt 2, 475-86.
- Fukuda, S., Fini, C. A., Mabuchi, T., Koziol, J. A., Eggleston, L. L., Jr. & Del Zoppo, G. J. 2004. Focal cerebral ischemia induces active proteases that degrade microvascular matrix. *Stroke*, 35, 4, 998-1004.
- Gaillard, P. J., Voorwinden, L. H., Nielsen, J. L., Ivanov, A., Atsumi, R., Engman, H., Ringbom, C., De Boer, A. G. & Breimer, D. D. 2001. Establishment and functional characterization of an in vitro model of the blood-brain barrier, comprising a co-culture of brain capillary endothelial cells and astrocytes. *Eur J Pharm Sci*, 12, 3, 215-22.
- Garcia, C. M., Darland, D. C., Massingham, L. J. & D'amore, P. A. 2004. Endothelial cell-astrocyte interactions and TGF beta are required for induction of blood-neural barrier properties. *Brain Res Dev Brain Res*, 152, 1, 25-38.
- Giulian, D., Baker, T. J., Shih, L. C. & Lachman, L. B. 1986. Interleukin 1 of the central nervous system is produced by ameboid microglia. *J Exp Med*, 164, 2, 594-604.
- Gohring, W., Sasaki, T., Heldin, C. H. & Timpl, R. 1998. Mapping of the binding of platelet-derived growth factor to distinct domains of the basement membrane proteins BM-40 and perlecan and distinction from the BM-40 collagen-binding epitope. *Eur J Biochem*, 255, 1, 60-6.
- Gordon, E. L., Danielsson, P. E., Nguyen, T. S. & Winn, H. R. 1991. A comparison of primary cultures of rat cerebral microvascular endothelial cells to rat aortic endothelial cells. *In Vitro Cell Dev Biol*, 27A, 4, 312-26.
- Hall, C. N., Reynell, C., Gesslein, B., Hamilton, N. B., Mishra, A., Sutherland, B. A., O'farrell, F. M., Buchan, A. M., Lauritzen, M. & Attwell, D. 2014. Capillary pericytes regulate cerebral blood flow in health and disease. *Nature*, 508, 7494, 55-60.

References

- Hallmann, R., Horn, N., Selg, M., Wendler, O., Pausch, F. & Sorokin, L. M. 2005. Expression and function of laminins in the embryonic and mature vasculature. *Physiol Rev*, 85, 3, 979-1000.
- Hamby, M. E., Uliasz, T. F., Hewett, S. J. & Hewett, J. A. 2006. Characterization of an improved procedure for the removal of microglia from confluent monolayers of primary astrocytes. *J Neurosci Methods*, 150, 1, 128-37.
- Hawkes, C. A., Gatherer, M., Sharp, M. M., Dorr, A., Yuen, H. M., Kalaria, R., Weller, R. O. & Carare, R. O. 2013. Regional differences in the morphological and functional effects of aging on cerebral basement membranes and perivascular drainage of amyloid-beta from the mouse brain. *Aging Cell*, 12, 2, 224-36.
- Hellstrom, M., Kalen, M., Lindahl, P., Abramsson, A. & Betsholtz, C. 1999. Role of PDGF-B and PDGFR-beta in recruitment of vascular smooth muscle cells and pericytes during embryonic blood vessel formation in the mouse. *Development*, 126, 14, 3047-55.
- Helms, H. C. & Brodin, B. 2014. Generation of primary cultures of bovine brain endothelial cells and setup of cocultures with rat astrocytes. *Methods Mol Biol*, 1135, 365-82.
- Hill, R. A., Tong, L., Yuan, P., Murikinati, S., Gupta, S. & Grutzendler, J. 2015. Regional Blood Flow in the Normal and Ischemic Brain Is Controlled by Arteriolar Smooth Muscle Cell Contractility and Not by Capillary Pericytes. *Neuron*, 87, 1, 95-110.
- Hoheisel, D., Nitz, T., Franke, H., Wegener, J., Hakvoort, A., Tilling, T. & Galla, H. J. 1998. Hydrocortisone reinforces the blood-brain properties in a serum free cell culture system. *Biochem Biophys Res Commun*, 247, 2, 312-5.
- Hynd, M. R., Scott, H. L. & Dodd, P. R. 2004. Glutamate-mediated excitotoxicity and neurodegeneration in Alzheimer's disease. *Neurochem Int*, 45, 5, 583-95.
- Igarashi, Y., Utsumi, H., Chiba, H., Yamada-Sasamori, Y., Tobioka, H., Kamimura, Y., Furuuchi, K., Kokai, Y., Nakagawa, T., Mori, M. & Sawada, N. 1999. Glial cell line-derived neurotrophic factor induces barrier function of endothelial cells forming the blood-brain barrier. *Biochem Biophys Res Commun*, 261, 1, 108-12.
- Jansson, D., Rustenhoven, J., Feng, S., Hurley, D., Oldfield, R. L., Bergin, P. S., Mee, E. W., Faull, R. L. & Dragunow, M. 2014. A role for human brain pericytes in neuroinflammation. *J Neuroinflammation*, 11, 104.
- Jaworski, T., Lechat, B., Demedts, D., Gielis, L., Devijver, H., Borghgraef, P., Duimel, H., Verheyen, F., Kugler, S. & Van Leuven, F. 2011. Dendritic degeneration, neurovascular defects, and inflammation precede neuronal loss in a mouse model for tau-mediated neurodegeneration. *Am J Pathol*, 179, 4, 2001-15.
- Jefferies, W. A., Brandon, M. R., Hunt, S. V., Williams, A. F., Gatter, K. C. & Mason, D. Y. 1984. Transferrin receptor on endothelium of brain capillaries. *Nature*, 312, 5990, 162-3.

- Kago, T., Takagi, N., Date, I., Takenaga, Y., Takagi, K. & Takeo, S. 2006. Cerebral ischemia enhances tyrosine phosphorylation of occludin in brain capillaries. *Biochem Biophys Res Commun*, 339, 4, 1197-203.
- Kirk, J., Plumb, J., Mirakhur, M. & McQuaid, S. 2003. Tight junctional abnormality in multiple sclerosis white matter affects all calibres of vessel and is associated with blood-brain barrier leakage and active demyelination. *J Pathol*, 201, 2, 319-27.
- Koh, J. Y. & Choi, D. W. 1991. Selective blockade of non-NMDA receptors does not block rapidly triggered glutamate-induced neuronal death. *Brain Res*, 548, 1-2, 318-21.
- Larochelle, C., Alvarez, J. I. & Prat, A. 2011. How do immune cells overcome the blood-brain barrier in multiple sclerosis? *FEBS Lett*, 585, 23, 3770-80.
- Lee, S. W., Kim, W. J., Choi, Y. K., Song, H. S., Son, M. J., Gelman, I. H., Kim, Y. J. & Kim, K. W. 2003. SSeCKS regulates angiogenesis and tight junction formation in blood-brain barrier. *Nat Med*, 9, 7, 900-6.
- Levine, S. M., Bilgen, M. & Lynch, S. G. 2013. Iron accumulation in multiple sclerosis: an early pathogenic event. *Expert Rev Neurother*, 13, 3, 247-50.
- Li, Y., Zhao, L., Fu, H., Wu, Y. & Wang, T. 2015. Ulinastatin suppresses lipopolysaccharide induced neuro-inflammation through the downregulation of nuclear factor-kappaB in SD rat hippocampal astrocyte. *Biochem Biophys Res Commun*, 458, 4, 763-70.
- Liu, R., Zhang, T. T., Wu, C. X., Lan, X. & Du, G. H. 2011. Targeting the neurovascular unit: development of a new model and consideration for novel strategy for Alzheimer's disease. *Brain Res Bull*, 86, 1-2, 13-21.
- Liu, W. Y., Wang, Z. B., Wang, Y., Tong, L. C., Li, Y., Wei, X., Luan, P. & Li, L. 2015. Increasing the Permeability of the Blood-brain Barrier in Three Different Models in vivo. *CNS Neurosci Ther*, 21, 7, 568-74.
- Loffek, S., Schilling, O. & Franzke, C. W. 2011. Series "matrix metalloproteinases in lung health and disease": Biological role of matrix metalloproteinases: a critical balance. *Eur Respir J*, 38, 1, 191-208.
- Mancardi, G. L., Perdelli, F., Rivano, C., Leonardi, A. & Bugiani, O. 1980. Thickening of the basement membrane of cortical capillaries in Alzheimer's disease. *Acta Neuropathol*, 49, 1, 79-83.
- Marchi, N. & Lerner-Natoli, M. 2012. Cerebrovascular Remodeling and Epilepsy. *Neuroscientist*.
- Marco, S. & Skaper, S. D. 2006. Amyloid beta-peptide1-42 alters tight junction protein distribution and expression in brain microvessel endothelial cells. *Neurosci Lett*, 401, 3, 219-24.
- Matsumoto, J., Takata, F., Machida, T., Takahashi, H., Soejima, Y., Funakoshi, M., Futagami, K., Yamauchi, A., Dohgu, S. & Kataoka, Y. 2014. Tumor necrosis factor-alpha-stimulated brain pericytes possess a unique cytokine and chemokine release profile and enhance microglial activation. *Neurosci Lett*, 578, 133-8.

References

- Mattsson, N., Tosun, D., Insel, P. S., Simonson, A., Jack, C. R., Jr., Beckett, L. A., Donohue, M., Jagust, W., Schuff, N. & Weiner, M. W. 2014. Association of brain amyloid-beta with cerebral perfusion and structure in Alzheimer's disease and mild cognitive impairment. *Brain*, 137, Pt 5, 1550-61.
- Mehta, A., Prabhakar, M., Kumar, P., Deshmukh, R. & Sharma, P. L. 2013. Excitotoxicity: bridge to various triggers in neurodegenerative disorders. *Eur J Pharmacol*, 698, 1-3, 6-18.
- Merlini, M., Meyer, E. P., Ulmann-Schuler, A. & Nitsch, R. M. 2011. Vascular beta-amyloid and early astrocyte alterations impair cerebrovascular function and cerebral metabolism in transgenic arcAbeta mice. *Acta Neuropathol*, 122, 3, 293-311.
- Merwin, J. R., Anderson, J. M., Kocher, O., Van Itallie, C. M. & Madri, J. A. 1990. Transforming growth factor beta 1 modulates extracellular matrix organization and cell-cell junctional complex formation during in vitro angiogenesis. *J Cell Physiol*, 142, 1, 117-28.
- Monson, N. L., Ireland, S. J., Ligocki, A. J., Chen, D., Rounds, W. H., Li, M., Huebinger, R. M., Munro Cullum, C., Greenberg, B. M., Stowe, A. M. & Zhang, R. 2014. Elevated CNS inflammation in patients with preclinical Alzheimer's disease. *J Cereb Blood Flow Metab*, 34, 1, 30-3.
- Nakagawa, S., Deli, M. A., Kawaguchi, H., Shimizudani, T., Shimono, T., Kittel, A., Tanaka, K. & Niwa, M. 2009. A new blood-brain barrier model using primary rat brain endothelial cells, pericytes and astrocytes. *Neurochem Int*, 54, 3-4, 253-63.
- Nakagomi, T., Kubo, S., Nakano-Doi, A., Sakuma, R., Lu, S., Narita, A., Kawahara, M., Taguchi, A. & Matsuyama, T. 2015. Brain vascular pericytes following ischemia have multipotential stem cell activity to differentiate into neural and vascular lineage cells. *Stem Cells*, 33, 6, 1962-74.
- Nishioku, T., Matsumoto, J., Dohgu, S., Sumi, N., Miyao, K., Takata, F., Shuto, H., Yamauchi, A. & Kataoka, Y. 2010. Tumor necrosis factor-alpha mediates the blood-brain barrier dysfunction induced by activated microglia in mouse brain microvascular endothelial cells. *J Pharmacol Sci*, 112, 2, 251-4.
- Noell, S., Wolburg-Buchholz, K., Mack, A. F., Beedle, A. M., Satz, J. S., Campbell, K. P., Wolburg, H. & Fallier-Becker, P. 2011. Evidence for a role of dystroglycan regulating the membrane architecture of astroglial endfeet. *Eur J Neurosci*, 33, 12, 2179-86.
- Ogunshola, O. O. 2011. In vitro modeling of the blood-brain barrier: simplicity versus complexity. *Curr Pharm Des*, 17, 26, 2755-61.
- Okoye, M. I. & Watanabe, I. 1982. Ultrastructural features of cerebral amyloid angiopathy. *Hum Pathol*, 13, 12, 1127-32.
- Ortiz, G. G., Pacheco-Moises, F. P., Macias-Islas, M. A., Flores-Alvarado, L. J., Mireles-Ramirez, M. A., Gonzalez-Renovato, E. D., Hernandez-Navarro, V. E., Sanchez-Lopez, A. L. & Alatorre-Jimenez, M. A. 2014. Role of the blood-brain barrier in multiple sclerosis. *Arch Med Res*, 45, 8, 687-97.

- Pardridge, W. M. 2015. Blood-brain barrier drug delivery of IgG fusion proteins with a transferrin receptor monoclonal antibody. *Expert Opin Drug Deliv*, 12, 2, 207-22.
- Park, L., Zhou, J., Zhou, P., Pistick, R., El Jamal, S., Younkin, L., Pierce, J., Arreguin, A., Anrather, J., Younkin, S. G., Carlson, G. A., Mcewen, B. S. & Iadecola, C. 2013. Innate immunity receptor CD36 promotes cerebral amyloid angiopathy. *Proc Natl Acad Sci U S A*, 110, 8, 3089-94.
- Patabendige, A. & Abbott, N. J. 2014. Primary porcine brain microvessel endothelial cell isolation and culture. *Curr Protoc Neurosci*, 69, 3 27 1-3 27 17.
- Patel, A., Toia, G. V., Colletta, K., Bradaric, B. D., Carvey, P. M. & Hendey, B. 2011. An angiogenic inhibitor, cyclic RGDfV, attenuates MPTP-induced dopamine neuron toxicity. *Exp Neurol*, 231, 1, 160-70.
- Paul, J., Strickland, S. & Melchor, J. P. 2007. Fibrin deposition accelerates neurovascular damage and neuroinflammation in mouse models of Alzheimer's disease. *J Exp Med*, 204, 8, 1999-2008.
- Pei, Z., Pang, H., Qian, L., Yang, S., Wang, T., Zhang, W., Wu, X., Dallas, S., Wilson, B., Reece, J. M., Miller, D. S., Hong, J. S. & Block, M. L. 2007. MAC1 mediates LPS-induced production of superoxide by microglia: the role of pattern recognition receptors in dopaminergic neurotoxicity. *Glia*, 55, 13, 1362-73.
- Pekny, M. & Nilsson, M. 2005. Astrocyte activation and reactive gliosis. *Glia*, 50, 4, 427-34.
- Perriere, N., Demeuse, P., Garcia, E., Regina, A., Debray, M., Andreux, J. P., Couvreur, P., Scherrmann, J. M., Tamsamani, J., Couraud, P. O., Deli, M. A. & Roux, F. 2005. Puromycin-based purification of rat brain capillary endothelial cell cultures. Effect on the expression of blood-brain barrier-specific properties. *J Neurochem*, 93, 2, 279-89.
- Poschl, E., Schlotzer-Schrehardt, U., Brachvogel, B., Saito, K., Ninomiya, Y. & Mayer, U. 2004. Collagen IV is essential for basement membrane stability but dispensable for initiation of its assembly during early development. *Development*, 131, 7, 1619-28.
- Qin, L., Liu, Y., Hong, J. S. & Crews, F. T. 2013. NADPH oxidase and aging drive microglial activation, oxidative stress, and dopaminergic neurodegeneration following systemic LPS administration. *Glia*, 61, 6, 855-68.
- Radu, M. & Chernoff, J. 2013. An in vivo assay to test blood vessel permeability. *J Vis Exp*, 73, e50062.
- Reichel, A., Begley, D. J. & Abbott, N. J. 2003. An overview of in vitro techniques for blood-brain barrier studies. *Methods Mol Med*, 89, 307-24.
- Reyahi, A., Nik, A. M., Ghiami, M., Gritli-Linde, A., Ponten, F., Johansson, B. R. & Carlsson, P. 2015. Foxf2 Is Required for Brain Pericyte Differentiation and Development and Maintenance of the Blood-Brain Barrier. *Dev Cell*, 34, 1, 19-32.
- Rezai-Zadeh, K., Gate, D. & Town, T. 2009. CNS infiltration of peripheral immune cells: D-Day for neurodegenerative disease? *J Neuroimmune Pharmacol*, 4, 4, 462-75.

- Rist, R. J., Romero, I. A., Chan, M. W., Couraud, P. O., Roux, F. & Abbott, N. J. 1997. F-actin cytoskeleton and sucrose permeability of immortalised rat brain microvascular endothelial cell monolayers: effects of cyclic AMP and astrocytic factors. *Brain Res*, 768, 1-2, 10-8.
- Roberts, J., Kahle, M. P. & Bix, G. J. 2012. Perlecan and the blood-brain barrier: beneficial proteolysis? *Front Pharmacol*, 3, 155.
- Rothstein, J. D., Dykes-Hoberg, M., Pardo, C. A., Bristol, L. A., Jin, L., Kuncl, R. W., Kanai, Y., Hediger, M. A., Wang, Y., Schielke, J. P. & Welty, D. F. 1996. Knockout of glutamate transporters reveals a major role for astroglial transport in excitotoxicity and clearance of glutamate. *Neuron*, 16, 3, 675-86.
- Rubin, L. L., Hall, D. E., Porter, S., Barbu, K., Cannon, C., Horner, H. C., Janatpour, M., Liaw, C. W., Manning, K., Morales, J. & Et Al. 1991. A cell culture model of the blood-brain barrier. *J Cell Biol*, 115, 6, 1725-35.
- Ryu, J. K. & McLarnon, J. G. 2009. A leaky blood-brain barrier, fibrinogen infiltration and microglial reactivity in inflamed Alzheimer's disease brain. *J Cell Mol Med*, 13, 9A, 2911-25.
- Sarin, H. 2010. Physiologic upper limits of pore size of different blood capillary types and another perspective on the dual pore theory of microvascular permeability. *J Angiogenes Res*, 2, 14.
- Sarkar, S., Raymick, J., Mann, D., Bowyer, J. F., Hanig, J. P., Schmued, L. C., Paule, M. G. & Chigurupati, S. 2014. Neurovascular changes in acute, sub-acute and chronic mouse models of Parkinson's disease. *Curr Neurovasc Res*, 11, 1, 48-61.
- Sastry, S. & Arendash, G. W. 1995. Time-dependent changes in iron levels and associated neuronal loss within the substantia nigra following lesions within the neostriatum/globus pallidus complex. *Neuroscience*, 67, 3, 649-66.
- Schildge, S., Bohrer, C., Beck, K. & Schachtrup, C. 2013. Isolation and culture of mouse cortical astrocytes. *J Vis Exp*, 71.
- Sengillo, J. D., Winkler, E. A., Walker, C. T., Sullivan, J. S., Johnson, M. & Zlokovic, B. V. 2013. Deficiency in mural vascular cells coincides with blood-brain barrier disruption in Alzheimer's disease. *Brain Pathol*, 23, 3, 303-10.
- Shayan, G., Choi, Y. S., Shusta, E. V., Shuler, M. L. & Lee, K. H. 2011. Murine in vitro model of the blood-brain barrier for evaluating drug transport. *Eur J Pharm Sci*, 42, 1-2, 148-55.
- Shepro, D. & Morel, N. M. 1993. Pericyte physiology. *FASEB J*, 7, 11, 1031-8.
- Shimizu, F., Sano, Y., Saito, K., Abe, M. A., Maeda, T., Haruki, H. & Kanda, T. 2012. Pericyte-derived glial cell line-derived neurotrophic factor increase the expression of claudin-5 in the blood-brain barrier and the blood-nerve barrier. *Neurochem Res*, 37, 2, 401-9.
- Siddharthan, V., Kim, Y. V., Liu, S. & Kim, K. S. 2007. Human astrocytes/astrocyte-conditioned medium and shear stress enhance the barrier properties of human brain microvascular endothelial cells. *Brain Res*, 1147, 39-50.

- Sixt, M., Engelhardt, B., Pausch, F., Hallmann, R., Wendler, O. & Sorokin, L. M. 2001. Endothelial cell laminin isoforms, laminins 8 and 10, play decisive roles in T cell recruitment across the blood-brain barrier in experimental autoimmune encephalomyelitis. *J Cell Biol*, 153, 5, 933-46.
- Smith, Q. R. & Rapoport, S. I. 1986. Cerebrovascular permeability coefficients to sodium, potassium, and chloride. *J Neurochem*, 46, 6, 1732-42.
- Sofroniew, M. V. 2009. Molecular dissection of reactive astrogliosis and glial scar formation. *Trends Neurosci*, 32, 12, 638-47.
- Sofroniew, M. V. 2015. Astrocyte barriers to neurotoxic inflammation. *Nat Rev Neurosci*, 16, 5, 249-63.
- Soma, T., Chiba, H., Kato-Mori, Y., Wada, T., Yamashita, T., Kojima, T. & Sawada, N. 2004. Thr(207) of claudin-5 is involved in size-selective loosening of the endothelial barrier by cyclic AMP. *Exp Cell Res*, 300, 1, 202-12.
- Sorokin, L. 2010. The impact of the extracellular matrix on inflammation. *Nat Rev Immunol*, 10, 10, 712-23.
- Stamatovic, S. M., Dimitrijevic, O. B., Keep, R. F. & Andjelkovic, A. V. 2006. Protein kinase Calpha-RhoA cross-talk in CCL2-induced alterations in brain endothelial permeability. *J Biol Chem*, 281, 13, 8379-88.
- Stamatovic, S. M., Keep, R. F. & Andjelkovic, A. V. 2008. Brain endothelial cell-cell junctions: how to "open" the blood brain barrier. *Curr Neuropharmacol*, 6, 3, 179-92.
- Takata, F., Dohgu, S., Matsumoto, J., Takahashi, H., Machida, T., Wakigawa, T., Harada, E., Miyaji, H., Koga, M., Nishioku, T., Yamauchi, A. & Kataoka, Y. 2011. Brain pericytes among cells constituting the blood-brain barrier are highly sensitive to tumor necrosis factor-alpha, releasing matrix metalloproteinase-9 and migrating in vitro. *J Neuroinflammation*, 8, 106.
- Tambuyzer, B. R., Ponsaerts, P. & Nouwen, E. J. 2009. Microglia: gatekeepers of central nervous system immunology. *J Leukoc Biol*, 85, 3, 352-70.
- Thanabalasundaram, G., Schneidewind, J., Pieper, C. & Galla, H. J. 2011. The impact of pericytes on the blood-brain barrier integrity depends critically on the pericyte differentiation stage. *Int J Biochem Cell Biol*, 43, 9, 1284-93.
- Thompson, W. L. & Van Eldik, L. J. 2009. Inflammatory cytokines stimulate the chemokines CCL2/MCP-1 and CCL7/MCP-3 through NFkB and MAPK dependent pathways in rat astrocytes [corrected]. *Brain Res*, 1287, 47-57.
- Thomsen, L. B., Burkhart, A. & Moos, T. 2015a. A Triple Culture Model of the Blood-Brain Barrier Using Porcine Brain Endothelial cells, Astrocytes and Pericytes. *PLoS One*, 10, 8, e0134765.
- Thomsen, M. S., Andersen, M. V., Christoffersen, P. R., Jensen, M. D., Lichota, J. & Moos, T. 2015b. Neurodegeneration with inflammation is accompanied by accumulation of iron and ferritin in microglia and neurons. *Neurobiol Dis*, 81, 108-18.
- Tigges, U., Boroujerdi, A., Welser-Alves, J. V. & Milner, R. 2013. TNF-alpha promotes cerebral pericyte remodeling in vitro, via a switch from alpha1 to alpha2 integrins. *J Neuroinflammation*, 10, 33.

References

- Tigges, U., Welser-Alves, J. V., Boroujerdi, A. & Milner, R. 2012. A novel and simple method for culturing pericytes from mouse brain. *Microvasc Res*, 84, 1, 74-80.
- Tilling, T., Korte, D., Hoheisel, D. & Galla, H. J. 1998. Basement membrane proteins influence brain capillary endothelial barrier function in vitro. *J Neurochem*, 71, 3, 1151-7.
- Timmer, N. M., Van Horsen, J., Otte-Holler, I., Wilhelmus, M. M., David, G., Van Beers, J., De Waal, R. M. & Verbeek, M. M. 2009. Amyloid beta induces cellular relocalization and production of agrin and glypican-1. *Brain Res*, 1260, 38-46.
- Timpl, R. 1989. Structure and biological activity of basement membrane proteins. *Eur J Biochem*, 180, 3, 487-502.
- Vivekanantham, S., Shah, S., Dewji, R., Dewji, A., Khatri, C. & Ologunde, R. 2015. Neuroinflammation in Parkinson's disease: role in neurodegeneration and tissue repair. *Int J Neurosci*, 125, 10, 717-25.
- Wang, Y., Jin, S., Sonobe, Y., Cheng, Y., Horiuchi, H., Parajuli, B., Kawanokuchi, J., Mizuno, T., Takeuchi, H. & Suzumura, A. 2014. Interleukin-1beta induces blood-brain barrier disruption by downregulating sonic hedgehog in astrocytes. *PLoS One*, 9, 10, e110024.
- Whitlock, J. M., Melrose, J. & Iozzo, R. V. 2008. Diverse cell signaling events modulated by perlecan. *Biochemistry*, 47, 43, 11174-83.
- Winkler, E. A., Sagare, A. P. & Zlokovic, B. V. 2014. The pericyte: a forgotten cell type with important implications for Alzheimer's disease? *Brain Pathol*, 24, 4, 371-86.
- Wolburg, H., Noell, S., Mack, A., Wolburg-Buchholz, K. & Fallier-Becker, P. 2009. Brain endothelial cells and the glio-vascular complex. *Cell Tissue Res*, 335, 1, 75-96.
- Wu, C., Ivars, F., Anderson, P., Hallmann, R., Vestweber, D., Nilsson, P., Robenek, H., Tryggvason, K., Song, J., Korpos, E., Loser, K., Beissert, S., Georges-Labouesse, E. & Sorokin, L. M. 2009. Endothelial basement membrane laminin alpha5 selectively inhibits T lymphocyte extravasation into the brain. *Nat Med*, 15, 5, 519-27.
- Yao, Y., Chen, Z. L., Norris, E. H. & Strickland, S. 2014. Astrocytic laminin regulates pericyte differentiation and maintains blood brain barrier integrity. *Nat Commun*, 5, 3413.
- Yousif, L. F., Di Russo, J. & Sorokin, L. 2013. Laminin isoforms in endothelial and perivascular basement membranes. *Cell Adh Migr*, 7, 1, 101-10.
- Yu, Y. J., Atwal, J. K., Zhang, Y., Tong, R. K., Wildsmith, K. R., Tan, C., Bien-Ly, N., Hersom, M., Maloney, J. A., Meilandt, W. J., Bumbaca, D., Gadkar, K., Hoyte, K., Luk, W., Lu, Y., Ernst, J. A., Scearce-Levie, K., Couch, J. A., Dennis, M. S. & Watts, R. J. 2014. Therapeutic bispecific antibodies cross the blood-brain barrier in nonhuman primates. *Sci Transl Med*, 6, 261, 261ra154.

- Yu, Y. J., Zhang, Y., Kenrick, M., Hoyte, K., Luk, W., Lu, Y., Atwal, J., Elliott, J. M., Prabhu, S., Watts, R. J. & Dennis, M. S. 2011. Boosting brain uptake of a therapeutic antibody by reducing its affinity for a transcytosis target. *Sci Transl Med*, 3, 84, 84ra44.
- Yurchenco, P. D. & Schittny, J. C. 1990. Molecular architecture of basement membranes. *FASEB J*, 4, 6, 1577-90.
- Zamanian, J. L., Xu, L., Foo, L. C., Nouri, N., Zhou, L., Giffard, R. G. & Barres, B. A. 2012. Genomic analysis of reactive astrogliosis. *J Neurosci*, 32, 18, 6391-410.
- Zarow, C., Barron, E., Chui, H. C. & Perlmutter, L. S. 1997. Vascular basement membrane pathology and Alzheimer's disease. *Ann N Y Acad Sci*, 826, 147-60.
- Zlokovic, B. V. 2011. Neurovascular pathways to neurodegeneration in Alzheimer's disease and other disorders. *Nat Rev Neurosci*, 12, 12, 723-38.

APPENDIX A. STUDY III

**Neurodegeneration with inflammation is accompanied by accumulation
of iron in microglia and neurons**

Published in *Neurobiology of Disease*, Volume 81, September 2015, Pages 108-118



Neurodegeneration with inflammation is accompanied by accumulation of iron and ferritin in microglia and neurons



Maj Schneider Thomsen, Michelle Vandborg Andersen¹, Pia Rægaard Christoffersen¹, Malene Duedal Jensen¹, Jacek Lichota, Torben Moos^{*}

Laboratory for Neurobiology, Biomedicine Group, Department of Health Science and Technology, Aalborg University, Aalborg, Denmark

ARTICLE INFO

Article history:

Received 8 November 2014

Revised 3 March 2015

Accepted 12 March 2015

Available online 20 March 2015

Keywords:

Ferritin
Hepcidin
Iron
Microglia
Monocyte
Neurodegeneration

ABSTRACT

Chronic inflammation in the substantia nigra (SN) accompanies conditions with progressive neurodegeneration. This inflammatory process contributes to gradual iron deposition that may catalyze formation of free-radical mediated damage, hence exacerbating the neurodegeneration. This study examined proteins related to iron-storage (ferritin) and iron-export (ferroportin) (aka metal transporter protein 1, MTP1) in a model of neurodegeneration. Ibotenic acid injected stereotactically into the striatum leads to loss of GABAergic neurons projecting to SN pars reticulata (SNpr), which subsequently leads to excitotoxicity in the SNpr as neurons here become vulnerable to their additional glutamatergic projections from the subthalamic nucleus. This imbalance between glutamate and GABA eventually led to progressive shrinkage of the SNpr and neuronal loss. Neuronal cell death was accompanied by chronic inflammation as revealed by the presence of cells expressing ED1 and CD11b in the SNpr and the adjacent white matter mainly denoted by the crus cerebri. The SNpr also exhibited changes in iron metabolism seen as a marked accumulation of inflammatory cells containing ferric iron and ferritin with morphology corresponding to macrophages and microglia. Ferritin was detected in neurons of the lesioned SNpr in contrast to the non-injected side. Compared to non-injected rats, surviving neurons of the SNpr expressed ferroportin at unchanged level. Analyses of dissected SNpr using RT-qPCR showed a rise in ferritin-H and -L transcripts with increasing age but no change was observed in the lesioned side compared to the non-lesioned side, indicating that the increased expression of ferritin in the lesioned side occurred at the post-transcriptional level. Hepcidin transcripts were higher in the lesioned side in contrast to ferroportin mRNA that remained unaltered. The continuous entry of iron-containing inflammatory cells into the degenerating SNpr and their subsequent demise is probably responsible for iron donation in neurodegeneration. This is accompanied by only a slight increase in neuronal ferritin and not ferroportin, which suggests that the iron-containing debris of dying inflammatory cells and degenerating neurons gets scavenged by invading macrophages and activated microglia to prevent an increase in neuronal iron.

© 2015 Elsevier Inc. All rights reserved.

Introduction

Conditions with progressive neurodegeneration in the substantia nigra (SN) like Parkinson's disease (PD) and pantothenate kinase-associated neurodegeneration (aka neurodegeneration with brain

iron accumulation (NBIA) formerly Hallervorden–Spatz disease) are accompanied by chronic inflammation (Hayflick et al., 2006; Rouault, 2013; Andersen et al., 2014; Zecca et al., 2004; Levi and Finazzi, 2014), which contributes to gradual deposition of iron in affected brain areas (Andersen et al., 2014). The chronic deposition of iron may catalyze formation of free-radical mediated damage, hence gradually exacerbating the neurodegenerative stage (Filomeni et al., 2012). A mechanism by which iron can accumulate in brain areas with neurodegeneration is through the accumulation of iron-containing inflammatory cells such as macrophages (Rathnasamy et al., 2013). The macrophages phagocytose damaged neurons and subsequently undergo apoptosis and deposit their iron in the extracellular space (Neher et al., 2011; Reif and Simmons, 1990; Wirenfeldt et al., 2007; Tabas et al., 2009; Rathnasamy et al., 2013). This may interfere with the otherwise healthy neurons causing reactive oxygen species (ROS)-mediated damages, ranging from acute interference with the neuronal cellular membrane

Abbreviations: BBB, blood–brain barrier; DAB, 3,3'-diaminobenzidine tetrahydrochloride; iNOS, inducible nitric oxide synthetase; KPBS, potassium phosphate-buffered saline; NBIA, neurodegeneration with brain iron accumulation; NO, nitric oxide; NTBI, non-transferrin bound iron; P, post-surgery; PD, Parkinson's disease; ROS, reactive oxygen species; SN, substantia nigra; SNpr, substantia nigra pars reticulata.

^{*} Corresponding author at: Laboratory for Neurobiology, Biomedicine Group, Department of Health Science and Technology, Fr. Bajers Vej 3B, 1.216, Aalborg University, DK-9220 Aalborg East, Denmark.

E-mail address: tmoos@hst.aau.dk (T. Moos).

¹ Equal contribution.

Available online on ScienceDirect (www.sciencedirect.com).

and rapid cell death to chronic changes like post-translational modification of neuronal proteins e.g., propagation of alpha-synuclein oligomer formation and subsequent aggregate formation (Uversky et al., 2001; Riedlerer, 2004).

We recently reviewed the handling of iron in brain regions with extensive iron accumulation (Andersen et al., 2014). Iron is probably released into the extracellular space from dying neurons, apoptotic macrophages that have migrated into the brain, and glial cells. Iron may bind to transferrin which then facilitates the uptake of iron in healthy neurons containing transferrin receptors. This uptake mechanism is expected to cease via down-regulation of the neuronal receptor in conditions with ample iron (Moos et al., 1998). Neurons also take up non-transferrin bound iron (NTBI) that is unlikely to be lower in iron excess (Pelizzoni et al., 2011, 2012). The neuronal uptake of NTBI will induce ferritin expression as a means to scavenge the iron accumulation (Rouault, 2013). As ferroportin excretes ferrous iron across the cellular membrane, neurons may regulate their iron content by excretion. Theoretically the neurons would also increase their expression of ferroportin in conditions with iron-overloading, as the ferroportin mRNA has an iron-responsive element (Zhang et al., 2009). Ferroportin is widely expressed in neurons of the CNS and is often co-expressed with transferrin receptors in neurons thought to contain large amounts of iron, e.g., neurons of the medial habenular nucleus and neurons of the interpeduncular nucleus (Moos and Rosengren Nielsen, 2006; Moos et al., 1998). Counteracting the significance of neuronal ferroportin in pathological conditions, hepcidin, which is a hormone secreted from hepatocytes in inflammatory conditions and known to post-translationally down-regulate the expression of ferroportin (Nemeth et al., 2004), could enter inflamed brain regions with a compromised blood–brain barrier (BBB), and hence impede the function of ferroportin (Andersen et al., 2014).

The aim of the present study was to investigate the expression of ferritin and ferroportin in an experimental *in vivo* model of neurodegeneration with inflammation in the brain (Sastry and Arendash, 1995). In this model, ibotenic acid, a glutamate agonist, is injected into the striatum, which leads to cell death among a great number of GABAergic neurons projecting to neurons of the substantia nigra pars reticulata (SNpr). In turn, this will result in an overstimulation of these SNpr neurons by glutamate projecting from neurons of the nucleus subthalamicus. Eventually, this imbalance between glutamate and GABA leads to the death of the SNpr neurons and chronic inflammation in this site remote in distance from the injection site of ibotenic acid. The resulting pathology of the SNpr is followed by a significant 42% increase in total iron when measured as milligram iron per milligram protein after 1 month (Sastry and Arendash, 1995). We hypothesized that the time dependent increase in cellular iron in the SNpr with chronic neurodegeneration and accompanying inflammation would lead to changes in ferroportin and ferritin levels to facilitate neuronal iron export and storage, respectively.

Materials and methods

Animals

Forty-six male Wistar rats (Charles River Laboratories, Wilmington, DE) weighing 250–300 g were housed in cages at the Animal Department of Aalborg University Hospital under constant temperature and humidity conditions and a 12 hour light/dark cycle with free access to food and water. The handling of the animals in this study was approved by the Danish Experimental Animal Inspectorate under the Ministry of Food and Agriculture.

Surgical procedure

Ibotenic acid was stereotactically injected in quadruplicate into the striatum, which leads to loss of GABAergic neurons in the striatum

including their fibers projecting to the SNpr (Fig. 1A) (Sastry and Arendash, 1995). The rats were anesthetized using hypnorm–dormicum (20 mg/100 g) injected subcutaneously and placed in a stereotactic apparatus. The skin was incised along the midline exposing the skull. Ibotenic acid (Sigma–Aldrich) was injected using a 10 μ l Hamilton Syringe in doses of 5 μ g dissolved in 1 μ l PBS into the left striatum at two depths in each drill hole at coordinates 0,35; 3,05; 4,2 and 5,5 mm (anterior; lateral; ventral) and –1,2; 3,65; 4,5 and 6,2 mm (anterior; lateral; ventral) relative to bregma using a stereotactic atlas for orientation (Paxinos and Watson, 1986).

Tissue preparation

At post-surgery (P) day 3 (n = 8), day 7 (n = 5), day 28 (n = 4), and day 91 (n = 8), the rats were euthanized with an overdose of hypnorm–dormicum injected subcutaneously and transcardially perfused via the left ventricle, first with saline and then with 4% paraformaldehyde in 0.01 M potassium phosphate-buffered saline (KPBS), pH 7.4. The brains were dissected and post-fixed in 4% paraformaldehyde overnight at 4 °C. A control group of non-injected rats was also included and examined corresponding to post-surgery days 3 (n = 3) and 91 (n = 8). Serial coronal sections (40 μ m) through striatum and SN were cut on a cryostat and collected free-floating in 0.1 M PBS, pH 7.4 in a sequential series of six. For RT-qPCR analyses, rats were euthanized with an overdose of hypnorm–dormicum injected subcutaneously at post-surgery interval day 91 (n = 4), and the brains rapidly dissected on ice under a dissecting microscope to isolate the ventral mesencephalon containing the SNpr from both the operated and non-operated sides. The ventral mesencephalon containing the SNpr from age-matched non-injected rats was similarly isolated bilaterally (n = 6).

Cresyl violet staining

Cresyl violet staining was used to quantify neurodegeneration. The sections were washed in KPBS three times and then immersed in a 0.5% gelatin solution, mounted on glass slides and dried. Subsequently, they were stained for 5 min in cresyl violet and rinsed in running tap water. The sections were then dehydrated in graded alcohols, dried and sealed in Pertex Mounting Media. To quantify the degeneration of the SNpr, the width was measured using the center of the interpeduncular nucleus as a reference of orientation. A horizontal line and a line at an angle of 45° through each SN were measured to divide the SNpr into a ventro-medial and a dorso-lateral part (Fig. 2A).

Immunohistochemistry

The sections were pre-incubated in blocking buffer consisting of 3% swine serum diluted in 0.01 M KPBS with 0.3% Triton X-100 (Sigma) for 30 min at room temperature to block any unspecific binding. The sections were then incubated overnight at 4 °C with primary antibodies diluted in blocking buffer: Mouse anti-rat CD11b (OX42) (Serotec) diluted 1:100, mouse anti-rat CD68 (ED1) (Abcam) diluted 1:100, rabbit anti-human ferritin (Dako) diluted 1:200, and rabbit-anti ferroportin (Abboud and Haile, 2000) diluted 1:1000. The polyclonal antibody raised against ferritin also reacts with both isotypes of rat ferritin (Hansen et al., 1999). Next day, the sections were incubated for 30 min at room temperature with biotinylated goat anti-mouse immunoglobulin (Dako) or biotinylated swine anti-rabbit immunoglobulin (Dako) both diluted 1:200 in KPBS. Binding of the antibodies was visualized using the ABC-system and 3,3'-diaminobenzidine tetrahydrochloride (DAB) (Moos et al., 2006).

Iron staining

The Prussian blue–DAB staining method was used to demonstrate ferric iron (Moos et al., 2006). In brief, sections were treated with 2%

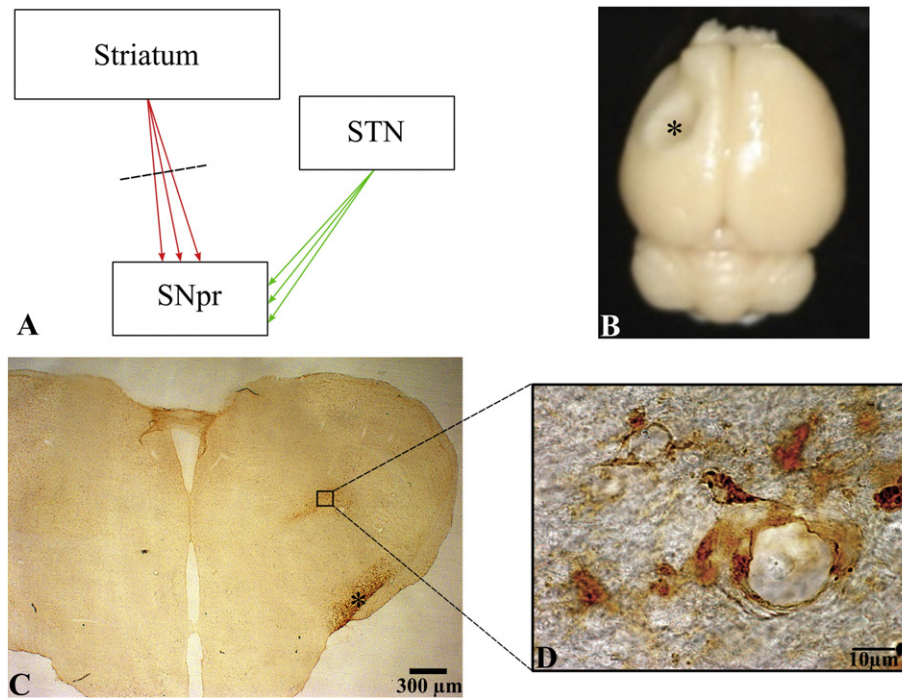


Fig. 1. Injection of ibotenic acid in striatum leads to neurodegeneration in substantia nigra pars reticulata (SNpr). A. SNpr receives dual innervation consisting of inhibitory GABAergic axons from striatum (red) and excitatory glutamatergic axons from the subthalamic nucleus (STN) (green). Chemical lesion of striatum causes over-stimulations of SNpr by the projections from STN which eventually leads to neurodegeneration accompanied by inflammation. B. The chemical lesion of striatal neurons with ibotenic acids leads to profound neuronal death, inflammation and eventual shrinkage of the brain corresponding to the region containing the striatum and overlying cerebral cortex, which is observable by the bare eye (asterisk). C. Increased ED1 immunolabeling in the diencephalon containing the projections from the striatum to the SNpr (square) on experimental day 91. The affected SNpr is also seen (asterisk). D. ED1 immunoreactive cells shown at high-power magnification from the area marked in C.

hydrochloric acid to release ferric ions from binding proteins. These ions then react with potassium ferrocyanide to produce the insoluble ferric ferrocyanide compound. To enhance the signal cells were post-intensified using DAB.

RT-qPCR

Total RNA was extracted from the dissected SNpr using the GeneJET RNA Purification Kit (Thermo Scientific) and treated with DNase I enzyme according to the manufacturer's protocol. DNA free RNA samples were used as a template for cDNA synthesis, which was carried out with the RevertAid Premium First Strand cDNA Synthesis Kit (Thermo Scientific). Quantitative RT-PCR was performed with primers specific for ferritin L (Ref. sequence: NM_031701.2, forward CTACAGGCTCTGTGAGGACTTGAC; reverse AGTAGGAAGCTGTAGCGGCAGTTTG), ferritin H (Ref. sequence: NM_031329.2, forward CTGACTATGCGGAAAGAGTCGACAG; reverse AGAGGAATCTCTGGGCTACTTCAG), ferroportin (Ref. sequence: NM_031591.1, forward ATTCTATAAGGACGATGCGCTGGTG; reverse GCTGTTCAAGTATCACGGTGCATTG), hepcidin (Ref. sequence: NM_022712.1, forward TGGATCAAGCCAGATCAGCATTCTC; reverse TTCTTCCTCATCTGCAGCCAGTTT), and β -actin (Ref. sequence: NM_031144.3, forward CCTCTGAACCTAAGGCCAACCGTGAA; reverse AGTGGTACGACCAGAGGCATACAGGG). β -Actin was used as a housekeeping control gene for normalization purpose. All primers were synthesized by TAG Copenhagen (DK). 1 μ L cDNA, and 10 pmol of each primer were used for every PCR reaction together with the Maxima™ SYBR Green qPCR Master Mix (Thermo Scientific) in a final reaction volume of 20 μ L. The reactions were run in Mx3000P instrument (Agilent) and the following program was used: 1 \times : 95 $^{\circ}$ C 10 min; 40 \times : 95 $^{\circ}$ C 30 s; 60 $^{\circ}$ C 30 s; 72 $^{\circ}$ C 30 s. All products were verified by the melting curve, which was made using a default program. The control reaction (RT-) was performed identically except for the fact that 1 μ L total RNA was used instead of cDNA as a template. The relative quantities of cDNA in the analyzed samples were calculated by the method of Pfaffl (Pfaffl, 2001).

Statistical analysis

Data were analyzed by the GraphPad Prism 5.0 software. Data were presented as mean \pm SEM and the difference among the means was determined using a one way ANOVA with Tukey's multiple comparisons post hoc test. A probability value of $p < 0.05$ was considered to be statistically significant.

Results

Neurodegeneration

Injection of ibotenic acid into the striatum leads to loss of GABAergic neurons in the striatum, including their fibers projecting to the SNpr (Fig. 1A) (Sastry and Arendash, 1995). This loss of the striatal neurons results in a robust shrinkage of the striatum and overlying cerebral cortex, which could be observed by the naked eye when brains were examined on experimental day 91 (Fig. 1B). Furthermore as a consequence of the loss of striatal neurons, the nigral neurons become vulnerable to glutamatergic projections from the subthalamic nucleus, which eventually leads to their progressive death and accompanying inflammation (Fig. 1A). In the rat, the ED1 immunoreactivity is predominantly expressed by monocytes that migrate into the brain during inflammation and transforms into phagocytotic macrophages that subsequently may undergo apoptosis and lease their metal content (Andersen et al., 2014). Accordingly, ED1 immunoreactive cells are virtually only detectable in brain regions with inflammation, which is in contrast to CD11b positive inflammatory cells that are seen in both resting and activated microglia, brain macrophages and monocytes. ED1 positive inflammatory cells were observed in both striatum and fibers projecting to the SNpr during the entire experimental period (Figs. 1C–D) and in the SNpr already from experimental day 3. The ED1 positive brain macrophages seen in the areas containing fibers projecting to the SNpr were

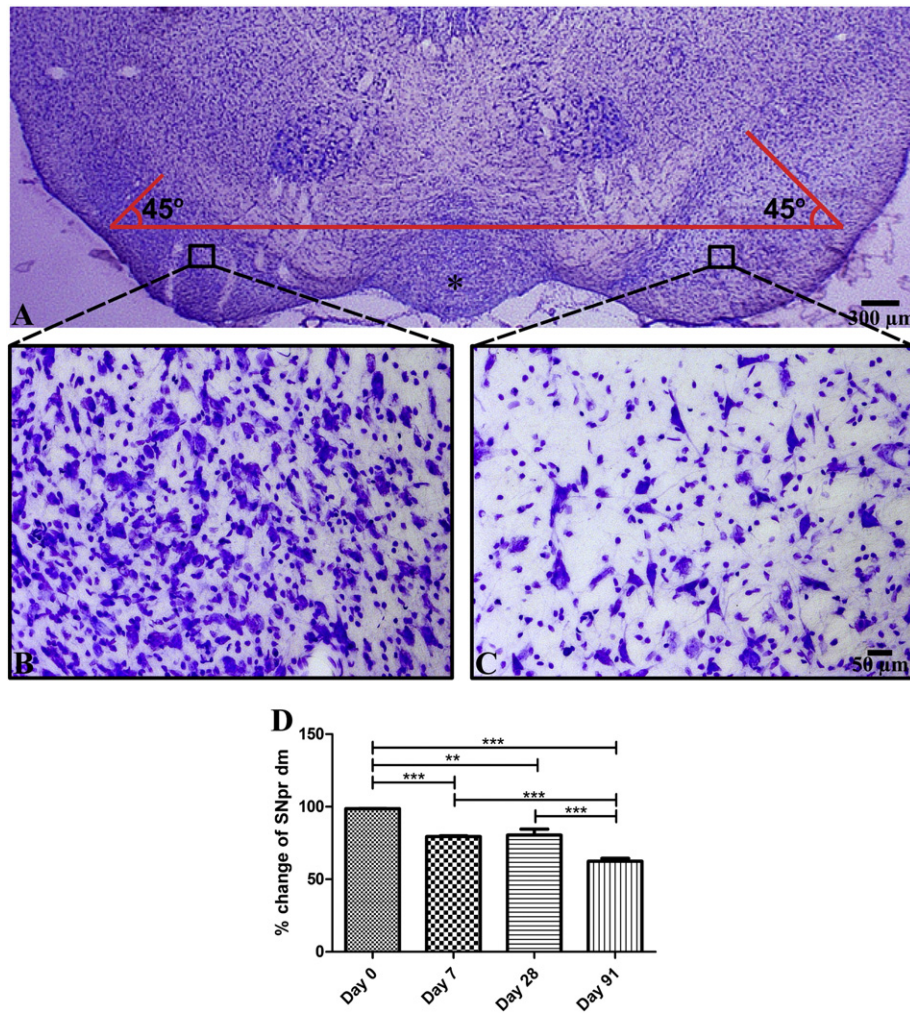


Fig. 2. Progressive neurodegeneration is observed in substantia nigra pars reticulata (SNpr). A. Standardized measurement of the SNpr. The interpeduncular nucleus marked with an asterisk was used as a reference point for laying a horizontal line perpendicular to a vertical line cutting through the cerebral aqueduct and the interpeduncular nucleus. An angle of 45° from this horizontal line cutting through the SNpr was used for measuring the width. B,C. The SNpr of the lesioned (B) and non-lesioned (C) sides shown at high magnification. The affected SNpr contains fewer neurons and a robust infiltration of inflammatory cells. D. When comparing the diameters (dm) of the SNpr between the lesioned and non-lesioned sides, it is evident that the diameter of the SNpr chronically shrinks. This is shown by the progressive decrease in the percentile difference between the diameters of the SNpr on the two sides. Data is represented as mean \pm SEM. ** $p < 0.001$; *** $p < 0.0001$.

often seen near post-capillary venules in good accordance with that the cells migrate into the brain via the transvascular route (c.f. Milligan et al., 1991). The chronic element of the degenerative process in the SNpr was also reflected in that a reduction in the size of this brain region occurred gradually during the post-surgery period (Fig. 2D). Hence, a significant decrease in the width of the SNpr measuring approximately 1 mm in the non-lesioned side (Paxinos and Watson, 1986) was observed, which reflected the maximal reduction in the SNpr (Fig. 2D). When examining the cresyl violet stained sections, the SNpr of the operated side contained fewer neurons compared to those of non-operated animals (Figs. 2B–C). The cresyl violet stained sections also contained multiple inflammatory cells identified by their small nuclei (Fig. 2B).

Neuroinflammation

The progressive neuronal death in the SNpr was accompanied by the presence of inflammatory cells that clearly exceeded the number present in the non-lesioned side throughout the experimental period as verified from the immunoreactivity of ED1 and CD11b immunoreactive cells being present in the lesioned SNpr already from experimental

day 3 (Figs. 3, 4). In the inflamed SNpr, the individual ED1 immunoreactive brain macrophages displayed signs of amoeboid cells probably reflecting their nature as monocytes that have migrated into the brain (Figs. 3F–G). The number of ED1 immunoreactive brain macrophages in the affected SNpr was slightly increased already from P3, but from then on the number increased and reached a maximum at the end of the observation period on post-surgical day 91 (Fig. 3E). This was clearly opposed in the absence of ED1 immunoreactive brain macrophages on the non-lesioned SNpr (Fig. 3F). The ED1 immunoreactive brain macrophages were also seen in the crus cerebri (Fig. 3G), which suggests that the macrophages migrated into the SNpr from the subarachnoid space beside from migrating through post-capillary venules. The crus cerebri of the non-lesioned side was unaffected (Fig. 3H). Like that seen with ED1, the number of activated CD11b immunopositive microglia in the affected SNpr was increased from P3 and remained elevated during the entire post-surgical period. The presence of inflammation in the crus cerebri was also evident when examining sections stained for CD11b immunoreactivity (Fig. 4). The individual CD11b immunoreactive microglia displayed signs of activation seen as retraction and hypertrophy of their peripheral processes, but the CD11b also displayed the morphology of migrating brain macrophages (Figs. 4F–G).

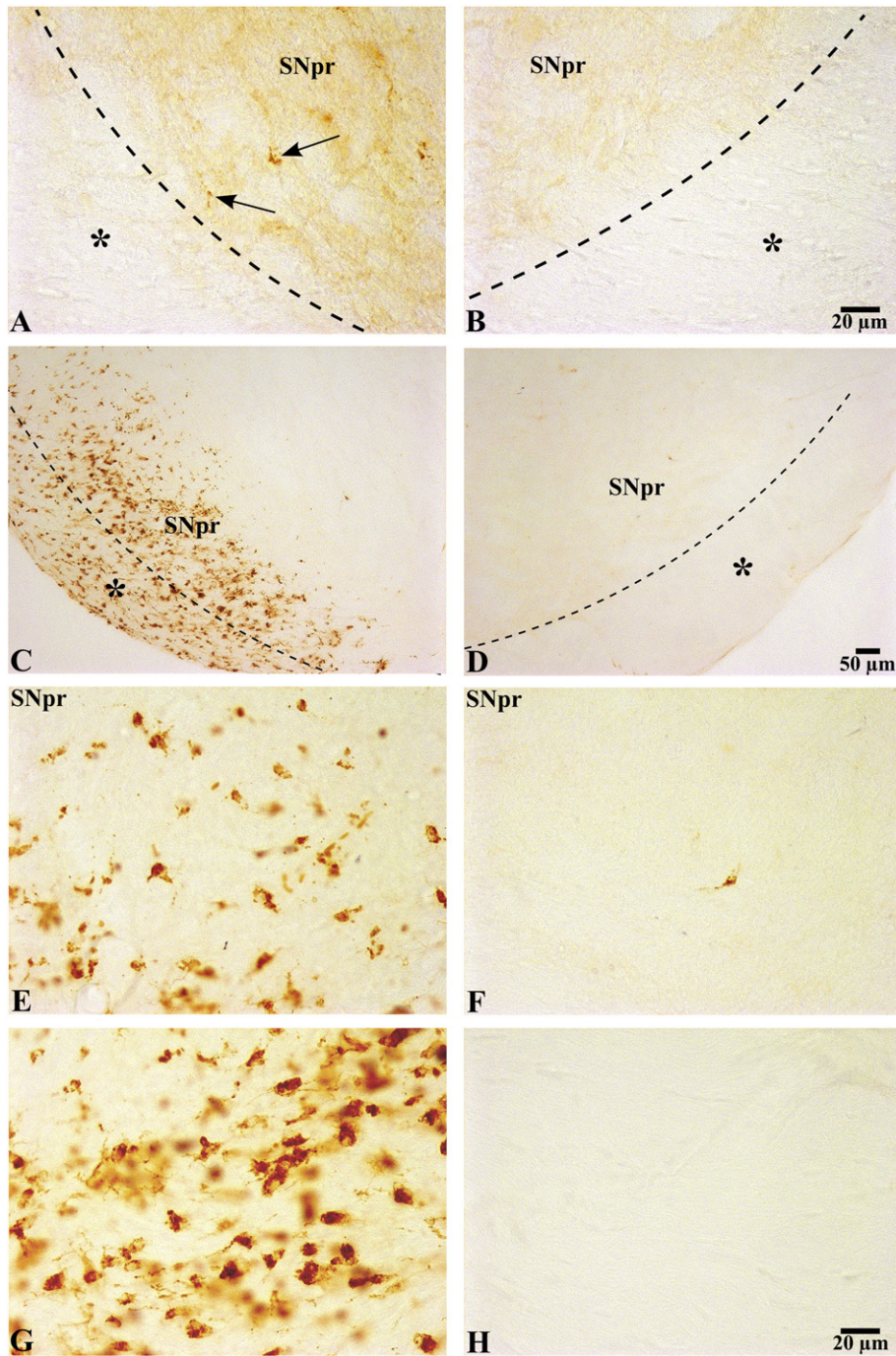


Fig. 3. Infiltration of ED1 immunoreactive cells in substantia nigra pars reticulata (SNpr) of the lesioned side. Representative pictures of sections from the substantia nigra pars reticulata (SNpr) showing ED1 immunoreactivity. Illustrations are taken on post-surgery days 3 (A,B), and 91 (C–H). Already from day 3, ED1 immunoreactivity is observed in the lesioned side (A, arrows), whereas the non-lesioned side is devoid of ED1 immunoreactivity (B), crus cerebri is marked with an asterisk. C,D. On experimental day 91, strong ED1 immunoreactivity is confined to the lesioned SNpr and the adjacent white matter of the crus cerebri (C, asterisk). This is clearly opposed in the absence of ED1 immunoreactivity on the non-lesioned side (D). The SNpr and crus cerebri of the lesioned (E,G) and non-lesioned (F,H) sides shown at high magnification. The non-lesioned side does not contain ED1 immunoreactivity in either SNpr (F) nor in crus cerebri (H). The ED1 immunoreactive inflammatory cells in the lesioned side are round or amoeboid in shape corresponding to their origin as brain macrophages that have migrated into the brain.

Iron metabolism

The distribution of iron, ferritin and ferroportin in the normal rat brain has been described in several publications (Benkovic and Connor, 1993; Burdo et al., 2001; Hill and Switzer, 1984; Moos and Rosengren Nielsen, 2006; Wu et al., 2004). In brief, histological iron and ferritin are detectable in the normal brain in glial cells like oligodendrocytes and resting microglia but not in neurons and astrocytes until

aging (Benkovic and Connor, 1993). The increase in total iron that occurs in the inflamed SNpr following injection of ibotenic acid (Sastry and Arendash, 1995) is therefore not followed by a general increase in histological detectable iron in all cells in this region. Ferroportin was seen in neurons and oligodendrocytes but not regularly in other glial cells. The distribution of histological iron and ferritin differed between the lesioned and non-lesioned sides in that cells with morphological similarity with brain macrophages and activated microglia could be

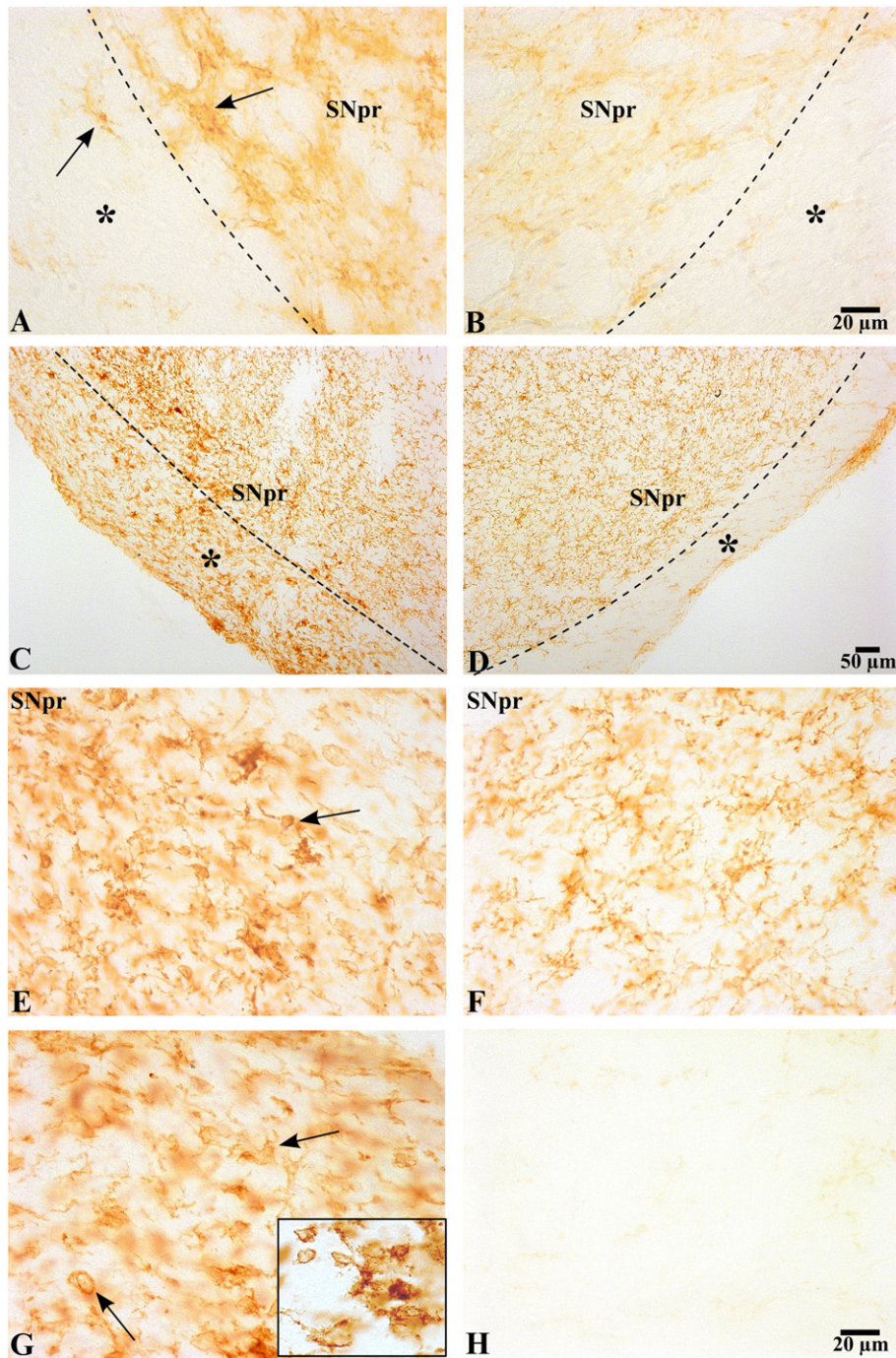


Fig. 4. Activated microglia cells can be observed in substantia nigra pars reticulata (SNpr) of the lesioned side. Representative pictures of sections from the SNpr showing CD11b immunoreactivity. Illustrations are taken on post-surgery days 3 (A,B), and 91 (C–H). Already from day 3, CD11b immunoreactivity is higher in the lesioned side (A, arrows) compared to the non-lesioned side that contains CD11b immunoreactive resting microglia (B). C–D. On experimental day 91, CD11b immunoreactivity is confined to the lesioned SNpr and the adjacent white matter of the crus cerebri (C, asterisk), the non-lesioned side contains resting microglia cells (D). The CD11b immunoreactivity in SNpr of the lesioned (E) and non-lesioned (F) sides shown at high magnification revealing activated round microglia cells in the lesioned side as indicated by the arrow. G. Crus cerebri of the lesioned side contains CD11b immunoreactivity. These cells are beside from being locally recruited and activated CD11b immunoreactive microglia cells, also CD11b immunoreactive inflammatory cells that are round or amoeboid in shape (arrows and inset) corresponding to their origin as brain macrophages that have migrated into the brain. H. The crus cerebri in the non-lesioned side is completely devoid of CD11b immunoreactivity.

seen in the inflamed SNpr (Figs. 5A,D). At the cellular level, the SNpr of the lesioned side dramatically differed in that iron was seen in cells with morphology corresponding to microglia and amoeboid macrophages and not in oligodendrocytes. These iron-positive microglia and macrophages were mostly observed in the SNpr and not in the crus cerebri (Fig. 5A). Iron was not detected in surviving neurons of the SNpr on the lesioned side. Ferritin immunolabeling was present among inflammatory cells with morphology corresponding to amoeboid

macrophages and microglia in both SNpr and the crus cerebri on the lesioned side (Figs. 5C–D). In contrast to that of iron, ferritin was also detected in cells with morphology corresponding to neurons on the lesioned side, especially on day 91 (Figs. 5F–G). In comparison with neurons, macrophages and microglia were however individually much more immunoreactive.

Ferroportin was seen in neurons of the mesencephalon in both the normal and the operated brain in regions like the oculomotor nucleus,

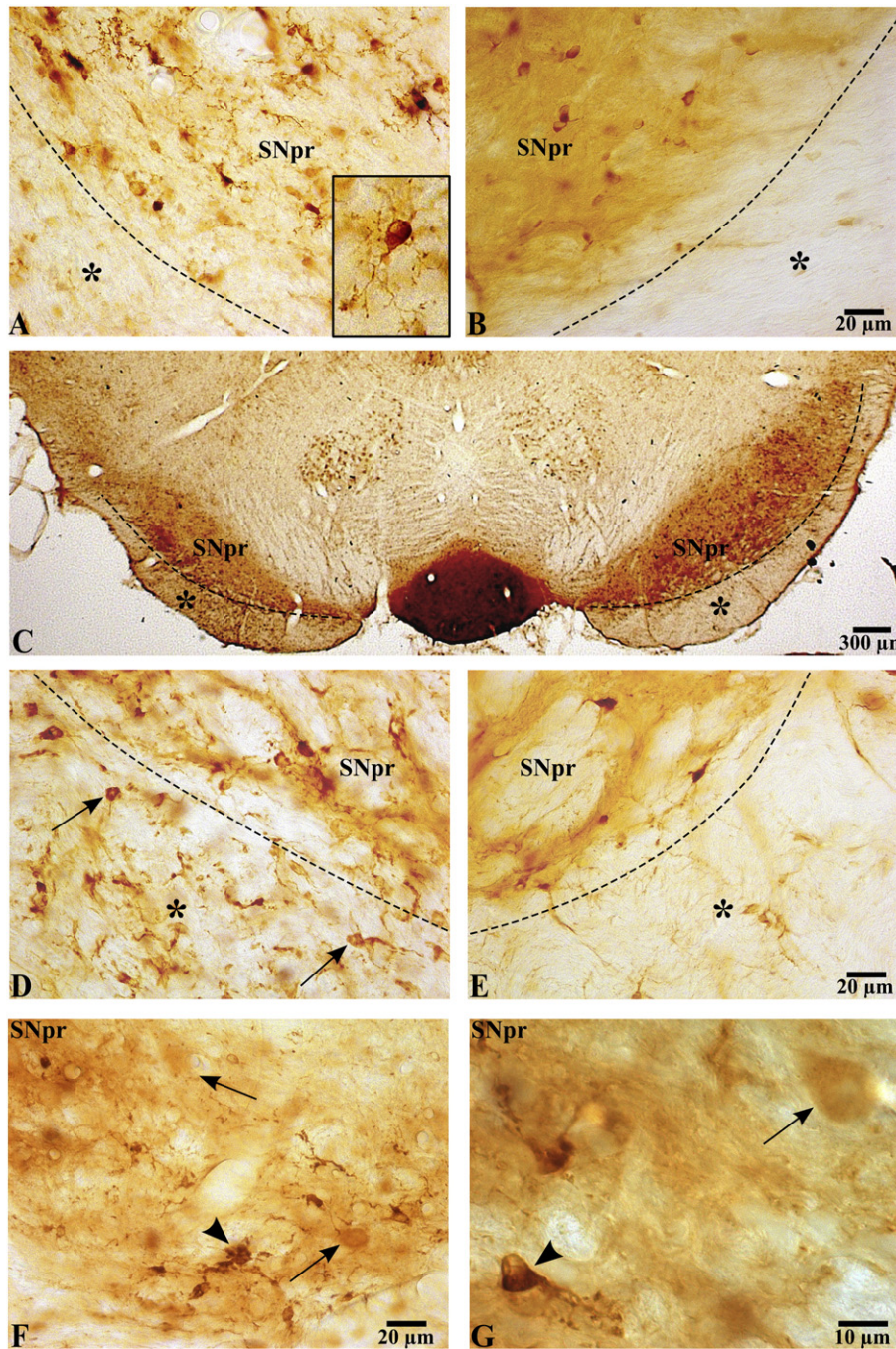


Fig. 5. Accumulation of ferric iron and ferritin in the lesioned substantia nigra pars reticulata (SNpr) and the white matter of the crus cerebri. Representative pictures of sections from SNpr showing histological detectable ferric iron (A,B) and ferritin immunoreactivity (C–G) on post-surgery day 91. In the lesioned side (A) ferric iron is present in the oligodendrocytes and cells with microglia cell morphology as highlighted in the inset, in the non-lesioned side (B) iron is confined to the oligodendrocytes and their ramifications. C. The altered iron-distribution is reflected in the ferritin immunolabeling in that the labeling is reduced in the SNpr but present in the white matter of the crus cerebri (asterisk) of the lesioned side (left) compared to the non-lesioned side (right). D,E. The SNpr and crus cerebri (asterisk) shown at higher magnification reveal the presence of round or amoeboid cells (arrows) in the crus cerebri of the lesioned side (D) corresponding to ferritin immunoreactive brain inflammatory cells that have migrated into the brain. There is barely any ferritin immunoreactivity in crus cerebri of the non-lesioned side (E). F,G. SNpr of the lesioned side shown at high magnification, revealing ferritin immunoreactivity in both neurons (arrows) and microglia cells (arrowheads).

red nucleus, and interpeduncular nucleus (Fig. 6A). In the SNpr and SNpc, the neurons were weakly labeled in the normal brain. In the lesioned side, ferroportin was not detected in cells with morphology corresponding to amoeboid macrophages or activated microglia. It was the clear impression that the number of neurons of the SNpr labeled with ferroportin was unaltered compared to the non-lesioned side (Figs. 6B–C), suggesting that the neurons did not upregulate their ferroportin expression or increased their content of ferroportin protein in response to the increase in iron.

RT-qPCR analyses of the dissected SNpr showed that transcripts of ferritin H and ferritin L were equally abundant in the rat brain on post-surgery days 0 and 91 when comparing the injected and non-injected sides. On day 91, both ferritin H and L were significantly higher expressed than on day 0. The expression of ferroportin was lower in the lesioned side on day 91 although this difference was non-significant when compared to the non-lesioned side. Hepcidin was significantly higher expressed on the lesioned side on day 91 (Fig. 7).

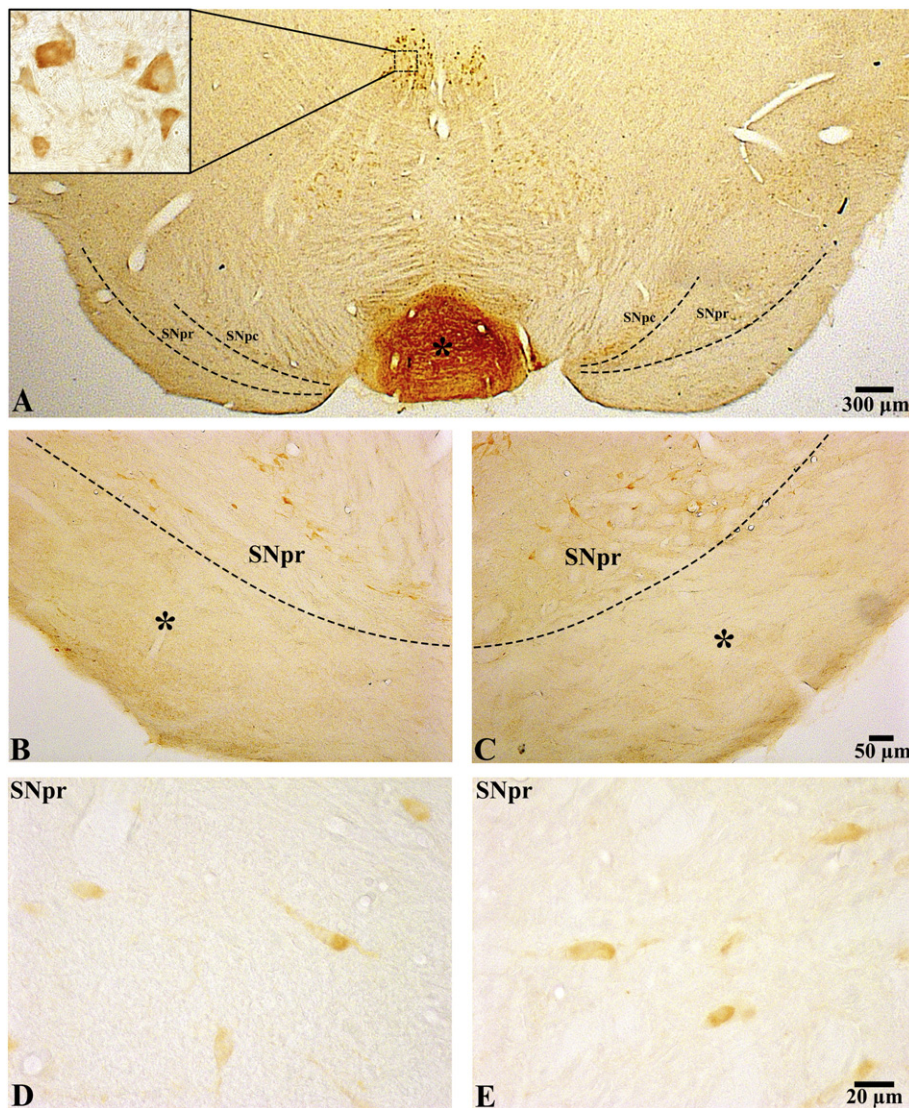


Fig. 6. Unchanged ferroportin expression in substantia nigra pars reticulata (SNpr) of the lesion side. A. Representative picture of section from the mesencephalon showing ferroportin immunoreactivity on post-surgery day 91 with the lesioned side shown to the left. The protein is present in neurons widespread in the mesencephalon like those of the oculomotor nucleus (A, inset) and interpeduncular nucleus (asterisk). Ferroportin immunoreactivity is also vaguely seen in neurons in the substantia nigra pars compacta (SNpc) and pars reticulata (SNpr). B–C. When shown at high magnification, it is apparent that ferroportin immunolabeling is seen lightly in neurons of the SNpr on both the lesioned (B) and non-lesioned (C) sides. Ferroportin is not seen in the white matter of the crus cerebri (asterisk). D,E. SNpr shown at high magnification, there is no apparent difference in the ferroportin immunoreactivity when comparing the lesioned (D) and non-lesioned sides (E).

Discussion

Experimental induced chronic neurodegeneration and inflammation

The excitotoxicity of the glutamatergic projections from the subthalamic nucleus denotes a powerful mechanism for neuronal cell death in the SNpr that can be prevented by supplying the GABA receptor agonist muscimol (Danbolt, 2001; Saji and Reis, 1987). Other contributing factors for neurodegeneration in the SNpr were the adjoining inflammatory process and iron-deposition. The affected SNpr and neighboring white matter revealed a chronic inflammatory process containing macrophages expressing ED1 and CD11b immunoreactive microglia during the entire observation period, including a dramatic inflammation even 91 days after injection of ibotenic acid, which signifies this experimental model for studies of chronic neurodegeneration with inflammation. The appearance of ED1 positive macrophages in adjacent white matter overlying the SNpr suggests that the macrophages entered the SNpr by chemoattraction subsequent to their migration into the subarachnoid space. The SNpr also revealed a change in iron metabolism seen as a

prominent content of inflammatory cells with morphology corresponding to macrophages and microglia cells containing ferric iron and ferritin. Iron-containing cells with morphology corresponding to microglia were only seen in the SNpr and not in the adjacent crus cerebri. There was a light tendency towards higher ferritin, but not of ferroportin, in neurons of the affected SNpr, which suggests that the resulting iron accumulation led to affection of scavenging inflammatory cells more than neurons. This notion gains support from the observation that macrophages and microglia were much more immunoreactive than neurons.

Macrophages can be characterized with respect to their detrimental (M1) or beneficial (M2) activity towards the diseased tissue (Kroner et al., 2014; c.f. Stoger et al., 2010). While true phenotypic markers of these two types are difficult to identify, the classification is relevant with respect to the macrophages' capability to synthesize nitric oxide (NO) as M1 and not M2. Inducible nitric oxide synthetase (iNOS) is an enzyme responsible for NO release in many pathological conditions of the brain with invasion of ED1 immunoreactive macrophages appearing in high density (Hernandez-Romero et al., 2012; Li et al., 2012; Pintado et al., 2011). NO interacts with the binding of iron to ferritin, as NO can

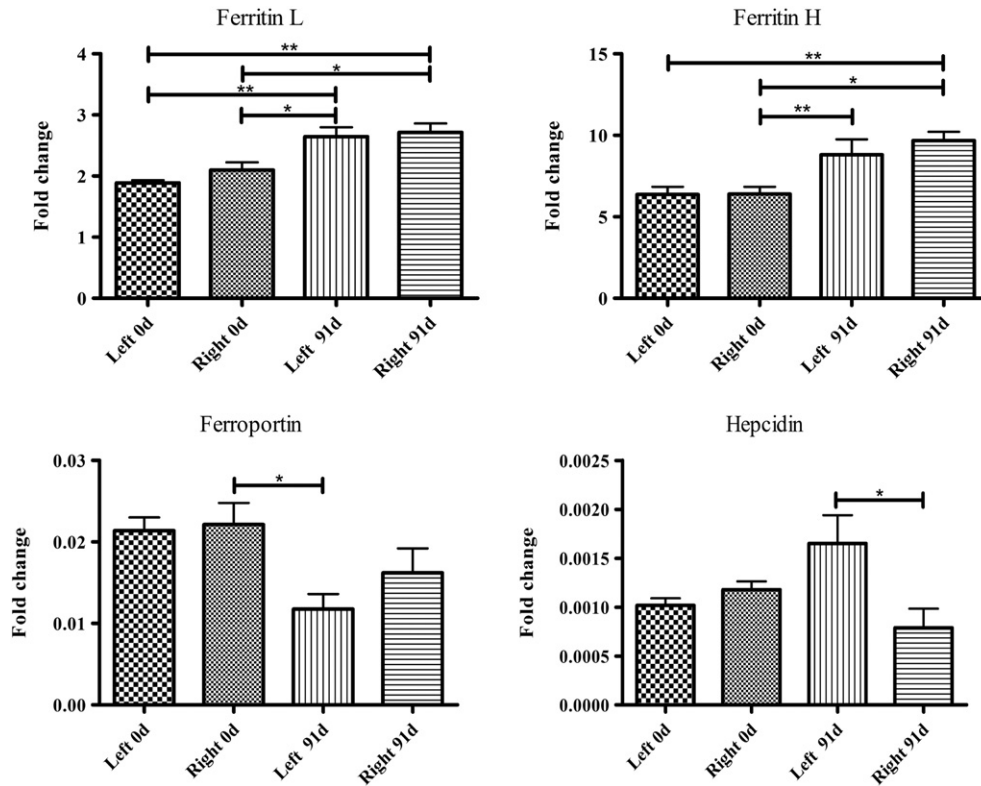


Fig. 7. Expression of ferritin L, ferritin H, ferroportin and hepcidin in substantia nigra pars reticulata (SNpr). RT-qPCR-analyses for ferritin L, ferritin H, ferroportin and hepcidin in substantia nigra pars reticulata on days 0 (non-operated) and 91 after injection. Left represents the lesioned side of the brain and right the non-lesioned side. There are significantly more ferritin transcripts in SNpr after 91 days, which may reflect that iron and ferritin post-transcriptionally increase in the brain with increasing age (Focht et al., 1997). There is no difference in the ferritin expression between the lesioned and non-lesioned sides on day 91. Ferroportin is lower in the operated side and overall lower on post-surgery day 91. There is significantly more hepcidin expressed in the lesioned side compared to the non-lesioned side on post-surgery day 91. The data are shown as fold change over actin and the data is represented as mean \pm SEM. * $p < 0.05$; ** $p < 0.001$.

release iron from ferritin causing iron to appear on reactive loosely bound forms (Reif and Simmons, 1990). Given the ample presence of iron and ferritin in the SNpr, the presence of iNOS positive M1 macrophages will make a strong contribution to amplifying the toxicity of iron. The inhibitor of iNOS aminoguanidine was shown to attenuate the neurotoxic effects of ferric iron injected directly into the ventricular system (Bostanci and Bagirci, 2008). Further studies analyzing the significance of NO released from macrophages in conditions with iron deposition in the brain are highly warranted, as inhibiting macrophages expressing iNOS could be beneficial to downscaling the effects of the continuous recruitment of M1 macrophages and their detrimental effects on the metabolism of iron (Li et al., 2012).

Iron management in neurodegeneration

In the human brain, neurons accumulate iron in areas affected by neurodegeneration (Dexter et al., 2011; Sofic et al., 1988). This accumulation may preferentially occur in intracellular aggregates and granules (Good et al., 1992a,b), which hardly occurs in the rodent brain during neurodegeneration. However, rodent neurons were also shown to accumulate iron to an extent that led to significant improvement when treated with an iron-chelator (Dexter et al., 2011). This would suggest that iron would accumulate intraneuronally and trigger expression of either ferritin for storage or ferroportin to increase the efflux. We observed a slight upregulation of ferritin in neurons on the lesioned side, whereas we were unable to detect iron in neurons. The latter observation was counteracted in the study of Sastry and Arendash (1995), who did find few neurons with histologically detectable iron in their observation period until four weeks after surgery. The detection sensitivity of the Prussian blue-DAB staining is clearly lower when compared to that of ferritin immunolabeling (Moos et al., 2006). Any differences in

iron detection could rely on that iron present in neurons could be on the limit of detection; but the presence of ferritin in neurons of the affected side as seen in the present study suggests that they have increased their iron content. The neurons may also incorporate iron by molecules non-detectable by the Prussian blue-DAB staining that mainly detects iron when present on its non-heme, ferric form (Moos et al., 2006).

Apart from causing possible damage to neurons due to intracellular accumulation and subsequent propagation of oxidative stress, iron is damaging in the vicinity of neurons when appearing on its ferrous form (Rouault, 2013; Andersen et al., 2014; Ward et al., 2014). Ferrous iron is thought to undergo rapid oxidation to ferric iron in biological systems, unless capacities are underscoring due to overproduction of ferrous iron as may occur in acute hemorrhage with lysis of red cells and degradation of heme from hemoglobin. The chronic inflammation did not find evidence for hemorrhage in spite of severe inflammation, but heme-containing proteins are likely to be released from demising macrophages and make their contribution to stress the capacity of anti-oxidants to prevent formation of free radicals. Ferrous iron is toxic in high concentrations due to an increased redox cycling (Jomova et al., 2010; Nunez et al., 2012), which will increase iron-catalyzed free radical formation that can induce neuronal damage by lipid peroxidation of cellular and organelle membranes, axonal dystrophy, and eventually necrosis and apoptotic cell death (Nunez et al., 2012; Rouault, 2013; Ward et al., 2014).

As iron accumulates in the brain bound to ferritin as a result of normal aging, ferritin detected in the SNpr of the lesioned side is not a result of the striatal lesion, but because the rats increased in age. The absence of differences in expression of ferritin H and L between the lesioned and non-lesioned sides does not preclude a higher level of ferritin as the accumulation of iron post-translationally increases synthesis of ferritin.

Ferritin transcripts were higher on day 91 compared to day 0, which is in good accordance with that ferritin expression increases in the brain with increasing age (Benkovic and Connor, 1993).

In addition to the participation of ferroportin in intestinal absorption and circulatory iron-homeostasis via expression in duodenal enterocytes, hepatocytes and macrophages, ferroportin is also expressed in neurons of the CNS with significant regional variations (Burdo et al., 2001; Moos and Rosengren Nielsen, 2006; Wu et al., 2004). Ferroportin is the only described protein known to mediate cellular efflux of iron, which would make mismatch in the functionality of ferroportin in the CNS a possibility for iron to get trapped inside neurons leading to their lack of capability to excrete iron. In turn this incapability to export iron from cells would lead to accumulation of iron inside CNS and pose neurons to an increased risk for ROS-mediated damage. However, despite that ferroportin was detectable in neurons of the SNpr, their immunoreactivity was however not higher than in the control side. This observation was confirmed in the RT-qPCR analysis wherein differences between the two sides were non-significant, although there was a tendency towards ferroportin being lower in the lesioned side, which can be explained by the loss of neurons in the SNpr.

Experimental neurodegeneration has never been correlated directly to changes in neuronal ferroportin expression, but injections of hepcidin into the lateral ventricle of rats lead to a decrease in neuronal ferroportin confirming the notion of a degradation of ferroportin in the presence of hepcidin (Wang et al., 2012). Hepcidin is synthesized mainly in the liver and to a lesser extent in monocytes ((Nguyen et al., 2006; Peyssonnaux et al., 2006; Theurl et al., 2008). Conversely, hepcidin is not synthesized in the brain unless in pathological conditions with inflammation (Urrutia et al., 2013; Simpson et al., 2015). Provided pathological condition within the CNS induces signaling in the circulation, it is predictable that such activity would subsequently induce hepcidin in plasma with the likelihood of passing into the brain if the integrity of the blood–brain barrier is compromised. Conditions with chronic pathology of the CNS leading to migration of iron-containing macrophages and their subsequent demise as discussed in previous paragraphs would make it likely that the neurons could suffer from the accumulation of iron released from dying macrophages combined with incapability to release iron via ferroportin due to the presence of hepcidin inside the inflamed CNS. Therefore the unaltered expression of ferroportin observed in the present examination in this model of chronic neurodegeneration could reflect a balance between a raise in ferroportin post-transcriptionally regulated by the readily iron access and a post-translational decrease due to hepcidin. Interestingly, iron deficient animals exhibit unaltered levels of ferroportin expression (Burdo et al., 2001; Wu et al., 2004), and no changes in the expression of ferroportin were found in mutated IRP2 mice in spite of regional increases in brain iron (Wu et al., 2004). These studies may indicate that robust changes in iron in the CNS would be needed to affect the ferroportin expression. Moreover, the data of the latter studies combined with the present also indicate that the regulation of neuronal iron levels is controlled via changes in ferritin gene translation in conditions with iron accumulation.

Conclusions

The neurodegenerative insult induced by excitotoxicity led to inflammation and accumulation of iron-containing microglia in the SNpr. The microglia probably act to scavenge excess iron originating from degrading neurons, glia and invading ferritin- and ED1-immunoreactive macrophages, but when their capacity is exceeded iron accumulates in the neurons as evinced from the larger content of neuronal ferritin. In contrast, no change in ferroportin expression was observed, which could be the result of counteracting regulation of its expression, i.e., increased post-transcriptionally expression via its regulation by IRE and a decreased post-translational expression via interaction with hepcidin at the cellular membrane.

Acknowledgments

This work was supported by grants from the Lundbeck Fund, the Danish Parkinson's Disease Fund, the Carlsberg Foundation, the Spar Nord Fond, and the Obelske Familiefond. We would like to thank Susan Peters at University of Copenhagen, Denmark and Merete Fredsgaard, Aalborg University, Denmark for their excellent technical assistance.

References

- Abboud, S., Haile, D.J., 2000. A novel mammalian iron-regulated protein involved in intracellular iron metabolism. *J. Biol. Chem.* 275, 19906–19912.
- Andersen, H.H., Johnsen, K.B., Moos, T., 2014. Iron deposits in the chronically inflamed central nervous system and contributes to neurodegeneration. *Cell. Mol. Life Sci.* 71, 1607–1622.
- Benkovic, S.A., Connor, J.R., 1993. Ferritin, transferrin, and iron in selected regions of the adult and aged rat brain. *J. Comp. Neurol.* 338, 97–113.
- Bostanci, M.O., Bagirici, F., 2008. Neuroprotective effect of aminoguanidine on iron-induced neurotoxicity. *Brain Res. Bull.* 76, 57–62.
- Burdo, J.R., Menzies, S.L., Simpson, I.A., Garrick, L.M., Garrick, M.D., Dolan, K.G., Haile, D.J., Beard, J.L., Connor, J.R., 2001. Distribution of divalent metal transporter 1 and metal transport protein 1 in the normal and Belgrade rat. *J. Neurosci. Res.* 66, 1198–1207.
- Danbolt, N.C., 2001. Glutamate uptake. *Prog. Neurobiol.* 65, 1–105.
- Dexter, D.T., Statton, S.A., Whitmore, C., Freinbichler, W., Weinberger, P., Tipton, K.F., Della Corte, L., Ward, R.J., Crichton, R.R., 2011. Clinically available iron chelators induce neuroprotection in the 6-OHDA model of Parkinson's disease after peripheral administration. *J. Neural Transm.* 118, 223–231.
- Filomeni, G., Bolaños, J.P., Mastroberardino, P.G., 2012. Redox status and bioenergetics liaison in cancer and neurodegeneration. *Int. J. Cell Biol.* 2012, 659645.
- Focht, S.J., Snyder, B.S., Beard, J.L., Van Gelder, W., Williams, L.R., Connor, J.R., 1997. Regional distribution of iron, transferrin, ferritin, and oxidatively-modified proteins in young and aged Fischer 344 rat brains. *Neuroscience* 79, 255–261.
- Good, P.F., Olanow, C.W., Perl, D.P., 1992a. Neuromelanin-containing neurons of the substantia nigra accumulate iron and aluminum in Parkinson's disease: a LAMMA study. *Brain Res.* 593, 343–346.
- Good, P.F., Perl, D.P., Bierer, L.M., Schmeidler, J., 1992b. Selective accumulation of aluminum and iron in the neurofibrillary tangles of Alzheimer's disease: a laser microprobe (LAMMA) study. *Ann. Neurol.* 31, 286–292.
- Hansen, T.M., Nielsen, H., Bernth, N., Moos, T., 1999. Expression of ferritin protein and subunit mRNAs in normal and iron deficient rat brain. *Mol. Brain Res.* 65, 186–197.
- Hayflick, S.J., Hartman, M., Coryell, J., Gitschier, J., Rowley, H., 2006. Brain MRI in neurodegeneration with brain iron accumulation with and without PANK2 mutations. *AJNR Am. J. Neuroradiol.* 27, 1230–1233.
- Hernandez-Romero, M.C., Delgado-Cortes, M.J., Sarmiento, M., De Pablos, R.M., Espinosa-Oliva, A.M., Arguelles, S., Bandez, M.J., Villaran, R.F., Maurino, R., Santiago, M., Venero, J.L., Herrera, A.J., Cano, J., Machado, A., 2012. Peripheral inflammation increases the deleterious effect of CNS inflammation on the nigrostriatal dopaminergic system. *Neurotoxicology* 33, 347–360.
- Hill, J.M., Switzer 3rd, R.C., 1984. The regional distribution and cellular localization of iron in the rat brain. *Neuroscience* 11, 595–603.
- Jomova, K., Vondrakova, D., Lawson, M., Valko, M., 2010. Metals, oxidative stress and neurodegenerative disorders. *Mol. Cell. Biochem.* 345, 91–104.
- Kroner, A., Greenhalgh, A.D., Zarruk, J.G., Passos Dos Santos, R., Gaestel, M., David, S., 2014. TNF and increased intracellular iron alter macrophage polarization to a detrimental M1 phenotype in the injured spinal cord. *Neuron* 83, 1098–1116.
- Levi, S., Finazzi, D., 2014. Neurodegeneration with brain iron accumulation: update on pathogenic mechanisms. *Front. Pharmacol.* 5, 99.
- Li, M., Dai, F.R., Du, X.P., Yang, Q.D., Chen, Y., 2012. Neuroprotection by silencing iNOS expression in a 6-OHDA model of Parkinson's disease. *J. Mol. Neurosci.* 48, 225–233.
- Milligan, C.E., Levitt, P., Cunningham, T.J., 1991. Brain macrophages and microglia respond differently to lesions of the developing and adult visual system. *J. Comp. Neurol.* 314, 136–146.
- Moos, T., Rosengren Nielsen, T., 2006. Ferroportin in the postnatal rat brain: implications for axonal transport and neuronal export of iron. *Semin. Pediatr. Neurol.* 13, 149–157.
- Moos, T., Oates, P.S., Morgan, E.H., 1998. Expression of the neuronal transferrin receptor is age dependent and susceptible to iron deficiency. *J. Comp. Neurol.* 398, 420–430.
- Moos, T., Skjoerringe, T., Gosk, S., Morgan, E.H., 2006. Brain capillary endothelial cells mediate iron transport into the brain by segregating iron from transferrin without the involvement of divalent metal transporter 1. *J. Neurochem.* 98, 1946–1958.
- Neher, J.J., Neniskyte, U., Zhao, J.W., Bal-Price, A., Tolkovsky, A.M., Brown, G.C., 2011. Inhibition of microglial phagocytosis is sufficient to prevent inflammatory neuronal death. *J. Immunol.* 186, 4973–4983.
- Nemeth, E., Tuttle, M.S., Powelson, J., Vaughn, M.B., Donovan, A., Ward, D.M., Ganz, T., Kaplan, J., 2004. Hepcidin regulates cellular iron efflux by binding to ferroportin and inducing its internalization. *Science* 306, 2090–2093.
- Nguyen, N.B., Callaghan, K.D., Ghio, A.J., Haile, D.J., Yang, F., 2006. Hepcidin expression and iron transport in alveolar macrophages. *Am. J. Physiol. Lung Cell. Mol. Physiol.* 291, L417–L425.
- Nunez, M.T., Urrutia, P., Mena, N., Aguirre, P., Tapia, V., Salazar, J., 2012. Iron toxicity in neurodegeneration. *Biometals* 25, 761–776.

- Paxinos, G., Watson, C., 1986. *The rat brain in stereotaxic coordinates*. Academic Press, San Diego.
- Pelizzoni, I., Macco, R., Morini, M.F., Zacchetti, D., Grohovaz, F., Codazzi, F., 2011. Iron handling in hippocampal neurons: activity-dependent iron entry and mitochondria-mediated neurotoxicity. *Aging Cell* 10, 172–183.
- Pelizzoni, I., Zacchetti, D., Smith, C.P., Grohovaz, F., Codazzi, F., 2012. Expression of divalent metal transporter 1 in primary hippocampal neurons: reconsidering its role in non-transferrin-bound iron influx. *J. Neurochem.* 120, 269–278.
- Peyssonnaud, C., Zinkernagel, A.S., Datta, V., Lauth, X., Johnson, R.S., Nizet, V., 2006. TLR4-dependent hepcidin expression by myeloid cells in response to bacterial pathogens. *Blood* 107, 3727–3732.
- Pfaffl, M.W., 2001. A new mathematical model for relative quantification in real-time RT-PCR. *Nucleic Acids Res.* 29, e45.
- Pintado, C., Revilla, E., Vizuete, M.L., Jimenez, S., Garcia-Cuervo, L., Vitorica, J., Ruano, D., Castano, A., 2011. Regional difference in inflammatory response to LPS-injection in the brain: role of microglia cell density. *J. Neuroimmunol.* 238, 44–51.
- Rathnasamy, G., Ling, E.A., Kaur, C., 2013. Consequences of iron accumulation in microglia and its implications in neuropathological conditions. *CNS Neurol Disord Drug Targets* 12, 785–798.
- Reif, D.W., Simmons, R.D., 1990. Nitric oxide mediates iron release from ferritin. *Arch. Biochem. Biophys.* 283, 537–541.
- Riedlerer, P.F., 2004. Views on neurodegeneration as a basis for neuroprotective strategies. *Med. Sci. Monit.* 10, RA287–RA290.
- Rouault, T.A., 2013. Iron metabolism in the CNS: implications for neurodegenerative diseases. *Nat. Rev. Neurosci.* 14, 551–564.
- Saji, M., Reis, D.J., 1987. Delayed transneuronal death of substantia nigra neurons prevented by gamma-aminobutyric acid agonist. *Science* 235, 66–69.
- Sastry, S., Arendash, G.W., 1995. Time-dependent changes in iron levels and associated neuronal loss within the substantia nigra following lesions within the neostriatum/globus pallidus complex. *Neuroscience* 67, 649–666.
- Simpson, I.A., Ponnuru, P., Klinger, M.E., Myers, R.L., Devraj, K., Coe, C.L., Lubach, G.R., Carruthers, A., Connor, J.R., 2015. A novel model for brain iron uptake: introducing the concept of regulation. *J. Cereb. Blood Flow Metab.* 35 (1), 48–57.
- Sofic, E., Riederer, P., Heinsen, H., Beckmann, H., Reynolds, G.P., Hebenstreit, G., Youdim, M.B., 1988. Increased iron (III) and total iron content in post mortem substantia nigra of parkinsonian brain. *J. Neural Transm.* 74, 199–205.
- Stoger, J.L., Goossens, P., De Winther, M.P., 2010. Macrophage heterogeneity: relevance and functional implications in atherosclerosis. *Curr. Vasc. Pharmacol.* 8, 233–248.
- Tabas, I., Seimon, T., Timmins, J., Li, G., Lim, W., 2009. Macrophage apoptosis in advanced atherosclerosis. *Ann. N. Y. Acad. Sci.* 1173 (Suppl. 1), E40–E45.
- Theurl, I., Theurl, M., Seifert, M., Mair, S., Nairz, M., Rumpold, H., Zoller, H., Bellmann-Weiler, R., Niederegger, H., Talasz, H., Weiss, G., 2008. Autocrine formation of hepcidin induces iron retention in human monocytes. *Blood* 111, 2392–2399.
- Urrutia, P., Aguirre, P., Esparza, A., Tapia, V., Mena, N.P., Arredondo, M., Gonzalez-Billault, C., Nunez, M.T., 2013. Inflammation alters the expression of DMT1, FPN1 and hepcidin, and it causes iron accumulation in central nervous system cells. *J. Neurochem.* 126, 541–549.
- Uversky, V.N., Li, J., Fink, A.L., 2001. Metal-triggered structural transformations, aggregation, and fibrillation of human alpha-synuclein. A possible molecular link between Parkinson's disease and heavy metal exposure. *J. Biol. Chem.* 276, 44284–44296.
- Wang, W., Fan, L., Xu, D., Wen, Z., Yu, R., Ma, Q., 2012. Immunotherapy for Alzheimer's disease. *Acta Biochim. Biophys. Sin. (Shanghai)* 44, 807–814.
- Ward, R.J., Zucca, F.A., Duyn, J.H., Crichton, R.R., Zecca, L., 2014. The role of iron in brain ageing and neurodegenerative disorders. *Lancet Neurol.* 13, 1045–1060.
- Wirenfeldt, M., Dissing-Olesen, L., Anne Babcock, A., Nielsen, M., Meldgaard, M., Zimmer, J., Azcoitia, I., Leslie, R.G., Dagnaes-Hansen, F., Finsen, B., 2007. Population control of resident and immigrant microglia by mitosis and apoptosis. *Am. J. Pathol.* 171, 617–631.
- Wu, L.J., Leenders, A.G., Cooperman, S., Meyron-Holtz, E., Smith, S., Land, W., Tsai, R.Y., Berger, U.V., Sheng, Z.H., Rouault, T.A., 2004. Expression of the iron transporter ferroportin in synaptic vesicles and the blood–brain barrier. *Brain Res.* 1001, 108–117.
- Zecca, L., Youdim, M.B., Riederer, P., Connor, J.R., Crichton, R.R., 2004. Iron, brain ageing and neurodegenerative disorders. *Nat. Rev. Neurosci.* 5, 863–873.
- Zhang, D.L., Hughes, R.M., Ollivierre-Wilson, H., Ghosh, M.C., Rouault, T.A., 2009. A ferroportin transcript that lacks an iron-responsive element enables duodenal and erythroid precursor cells to evade translational repression. *J. Biol. Chem.* 284, 461–473.

ISSN (online): 2246-1302
ISBN (online): 978-87-7112-446-0

AALBORG UNIVERSITY PRESS